

REMARKS

Claims 1-20 are pending in the application. Claims 12, 13, and 17-20 are withdrawn as being drawn to non-elected inventions. Applicants reserve the right to prosecute the non-elected claims in subsequent divisional applications. The Examiner states that claims 1-11 and 14 are currently being examined on the merits. Applicants respectfully request clarification as to the status of claims 15 and 16, which are not listed either as withdrawn or under examination.

The Examiner is respectfully reminded that, upon allowance of the antibody claims (1-11 and 14) claims 12-13 and 15-20, directed to processes for using same, must be rejoined. See the Commissioner's Notice in the Official Gazette of March 26, 1996, entitled "Guidance on Treatment of Product and Process Claims in light of *In re Ochiai*, *In re Brouwer* and 35 U.S.C. § 103(b)" which sets forth the rules, upon allowance of product claims, for rejoinder of process claims covering the same scope of products.

Claim 1 has been amended to further clarify the intended scope of the claimed subject matter. No new matter is added by this amendment. Entry of this amendment is respectfully requested.

Priority:

The Examiner asserts that neither of the parent applications contain support for a naturally occurring amino acid sequence having at least 90% sequence identity to SEQ ID NO:2, and that therefore claims drawn to this embodiment will be given priority to the instant filing date.

Claim 1 has been amended herein to further clarify the intended scope of the claimed subject matter. As amended herein, claim 1 recites "a naturally occurring human variant of SEQ ID NO:1." The phrase "naturally occurring" is defined in the specification at page 5, lines 15-16 as "an amino acid sequence which is found in nature." SCAH sequences are preferably from human, as disclosed at page 5, lines 12-13. Variants of SCAH are described at page 5, lines 17-24, and at page 12, lines 10-17. Thus all the elements of the claimed embodiment of the invention are described in the original specification as filed.

Furthermore, the specification discloses that sequences which encode SCAH variants are capable of hybridizing to the nucleotide sequence of the naturally occurring scah (that is, SEQ ID

NO:4) under appropriate conditions of stringency (page 8, lines 11-13). Polynucleotide sequences capable of hybridizing to SEQ ID NO:4 under various conditions of stringency are clearly disclosed as being within the scope of the invention at page 11, lines 13-15. The conditions which define various levels of stringency are defined at page 11, lines 20-25. The specification discloses that an intermediate specificity hybridization can be used to identify “similar or related polynucleotide sequences” (page 11, lines 24-25), which would include those encoding SCAH variants. This disclosure provides additional support for the recited variants of SEQ ID NO:2.

Accordingly, acknowledgment that the instant application is entitled to its priority date of July 3, 1996, for all the claimed subject matter is respectfully requested.

Rejections under 35 U.S.C. § 112, second paragraph:

Claims 1, 2, 9-11, and 14 are rejected under 35 U.S.C. § 112, second paragraph, as allegedly being indefinite. In particular, the Office Action asserts that the term “biologically active” is not defined in the specification.

Claim 1, as amended herein, no longer recites antibodies which bind to biologically active fragments of SEQ ID NO:2. The claims still recite antibodies to immunologically active fragments, which may have additional biological activities besides immunogenicity, but are not required to.

Withdrawal of the rejection under 35 U.S.C. § 112, second paragraph is respectfully requested.

Enablement rejections under 35 U.S.C. § 112, first paragraph:

Claims 1-11 and 14 are rejected under 35 U.S.C. § 112, first paragraph as allegedly lacking enablement. In particular, the Office Action asserts that “in order to make the claimed antibodies it is necessary to raise antibodies to all possible fragments of SEQ ID NO:2 of at least 10 residues and test the multitude of antibodies which would result from the experiments against a multitude of other proteins in order to determine if the antibody does indeed bind specifically to SEQ ID NO:2 without cross reactivity to other proteins” (Office Action, page 4). The Office Action concludes that this represents undue experimentation.

Applicants respectfully point out that the described experimentation does not reflect the process that would actually be carried out by one of skill in the art. In the first place, the skilled artisan would recognize that a specific antibody is not one which has no cross reactivity with anything else, but one which recognizes a specific antigen. For example, an excerpt from a textbook on immunology (Kimball, J.W., Introduction to Immunology, 2nd Ed., Macmillan Publishing Company, New York, 1986; Reference No. 1, enclosed) defines the specificity of an antibody molecule as "its ability to discriminate between the antigenic determinant to which it was elicited and other antigenic determinants of a related structure" (Kimball, page 75). In describing an example of specific antibodies, Kimball concludes that "while these antibodies do show cross-reactivity, the reduced reaction with heterologous ligands reveals a substantial degree of specificity." (Kimball, page 76). Thus an antibody that specifically binds to SEQ ID NO:2 is not one which does not bind at all to any other proteins, as suggested in the Office Action (page 4), but one which binds better to a SEQ ID NO:2-specific epitope than to other epitopes.

Accordingly, in order to generate an antibody specific to SEQ ID NO:2, one of skill in the art need only select as immunogenic epitopes those fragments of at least 10 amino acid residues of SEQ ID NO:2 that are unique to SEQ ID NO:2. This selection can easily be done using computational search methods to compare SEQ ID NO:2 against publicly available protein databases. There is no need to test all other fragments that do not meet this simple criterion. Since the immunological epitope would not be shared by any protein other than SEQ ID NO:2, the antibody would inevitably be specific for SEQ ID NO:2.

The Office Action also cites Seaver to the effect that additional work with clinical specimens is needed to insure selection of a monoclonal antibody suitable for clinical diagnosis. Applicants respectfully note that the claimed antibodies are useful even if they are not perfectly suitable for clinical diagnosis, for example, in the purification of SCAH-2 protein (specification, page 43, lines 17-28), or in the drug screening techniques described in the specification at page 23 line 27 through page 24 line 2. Moreover, the Paul reference cited in the Office Action discloses that polyclonal antibodies (as in claims 3-5) can have greater specificity than a monoclonal antibody, and that a combination of monoclonal antibodies may be the best of all (Paul, page 460, col. 2). Thus the art suggests that the

claimed antibodies are useful as diagnostics without any further experimentation. In addition, the fact that methods for selecting monoclonal antibodies for clinical diagnosis were well known in the art before the time of filing, as shown by the Seaver reference, demonstrates that the experimentation needed to produce such antibodies was not undue.

Applicants also respectfully direct the Examiner's attention to the enclosed postfiling references describing uses for monoclonal antibodies to prostate stem cell antigen (PSCA). As previously discussed in the Preliminary Remarks filed August 23, 2001, PSCA has 99% amino acid sequence identity to SEQ ID NO:2, differing only at the position of the "X" residue in SEQ ID NO:2. The Preliminary Remarks also discussed the Saffran reference (Saffran, D.C. et al., "Anti-PSCA mAbs inhibit tumor growth and metastasis formation and prolong the survival of mice bearing human prostate cancer xenografts" Proc. Natl. Acad. Sci. USA (2001) 98:2658-2663 (Reference No. 2, enclosed)). This postfiling reference demonstrated that anti-PSCA monoclonal antibodies could be successfully used to inhibit tumor formation in mice (Saffran, page 2658, col. 2). There was no mention of cross-reactivity to other targets, and the mice remained healthy and active during treatment (Saffron, page 2662, col. 1), indicating that there were no unwanted side effects due to cross-reactivity to other proteins.

The Examiner's attention is also directed to the Amara reference (Amara, N. et al., "Prostate stem cell antigen is overexpressed in human transitional cell carcinoma" Cancer Res. (2001) 61:4660-4665 (Reference No. 3, enclosed)). The Amara reference discloses the use of an anti-PSCA monoclonal antibody to detect PSCA expression in bladder tumor tissues. Increasing levels of PSCA detected correlated with increasing tumor grade (Amara, page 4663, col. 2), indicating that there was no significant cross-reactivity to confuse the results. The Ross reference (Ross, S. et al., "Prostate stem cell antigen as therapy target: Tissue expression and in vivo efficacy of a immunoconjugate" Cancer Res. (2002) 62:2546-2553 (Reference No. 4, enclosed)) discloses the production of anti-PSCA monoclonal antibodies for use in immunotherapy. Three different monoclonal antibodies were generated that specifically recognized human PSCA, with no cross-reactivity to mouse PSCA (Ross, page 2549, col.1). Thus the postfiling art confirms that those of skill in the art would not in fact have

difficulty in generating monoclonal antibodies specific to SEQ ID NO:2 that would be useful in both diagnostic and therapeutic methods.

For at least the above reasons, withdrawal of the enablement rejections under 35 U.S.C. § 112, first paragraph is respectfully requested.

Rejections under 35 U.S.C. § 102:

Claims 1, 2, and 6-8 are rejected under 35 U.S.C. § 102(b) as allegedly being anticipated by Blake et al. Blake et al. describe an antibody which binds to the Ly-6 antigen. The Office Action asserts that because SCAH-2 is a member of the Ly-6 family and conserves protein sequences important for tertiary structure, the Blake antibody would cross-react with SCAH-2.

Applicants first note that, as discussed in the previous section, cross-reactivity does not equal specificity; an antibody that specifically binds to SEQ ID NO:2 or a variant or fragment thereof is one which recognizes a specific epitope of SEQ ID NO:2. There is no evidence that the mouse Ly-6 protein of Blake et al. shares any antigenic determinants with SEQ ID NO:2. Applicants respectfully point out that the mouse Ly-6A.2/E.1 protein, to which the Blake antibodies specifically bound (Blake, page 1141, col. 1), shares only 17% amino acid sequence identity with SEQ ID NO:2 (see the sequence alignment attached as Exhibit A). The longest contiguous fragment that is shared by the two proteins is only 4 amino acids in length. Thus the Blake antibodies clearly do not anticipate the claimed antibodies that specifically bind to fragments of at least 10 amino acids of SEQ ID NO:2, because the Blake protein contains no such fragments which the antibodies could have recognized.

Applicants also respectfully point out that the Paul reference cited in the Office Action discloses that the three dimensional structure of a protein is one component that defines an antigenic determinant, in addition to the actual amino acid residues involved (Paul, page 243, col. 1). For this reason, a protein which shares the three dimensional structure of another protein, but has different amino acid residues on its surface, would not share antigenic determinants. Given that only 17% of the amino acid residues (only 28 in all) are conserved between SCAH-2 and Ly-6, it is highly unlikely that enough of these conserved residues have clustered together on the surface of the protein so as to produce a conserved antigenic determinant. This is particularly unlikely given that almost all of the conserved

residues are hydrophobic residues that are likely to be buried in the interior of the protein and therefore unavailable for binding to antibodies. Note that the specification points out that it is hydrophilic regions which make appropriate epitopes (specification, page 43, lines 6-8). Furthermore, Applicants note that, as disclosed in the Ross reference, even antibodies to the same PSCA protein from different species (much less a distant family member from another species) do not cross-react (Ross, page 2549, col. 1). Thus it is not at all reasonable to conclude that the antibody described by Blake et al. would bind to SCAH-2 at all, much less bind specifically to SCAH-2.

The Office Action further asserts that claims 1-9 and 14 are anticipated by Reiter et al. Applicants respectfully point out that the Reiter patent has a priority date of March 10, 1997, considerably after the instant application's priority date of July 3, 1996. In fact, the Reiter patent cites to the instant application's priority patent, U.S. Patent No. 5,856,136. As discussed above, the instant application is entitled to its priority date for the recited antibodies. Thus the Reiter patent is not prior art with respect to the instant claims.

Withdrawal of the rejections under 35 U.S.C. § 102 is therefore respectfully requested.

Rejections under 35 U.S.C. § 103:

Claims 3-5 are rejected under 35 U.S.C. § 103(a) as allegedly being obvious over Blake et al, in view of Paul. As discussed above, Blake et al. does not anticipate the claimed monoclonal antibodies, as it does not disclose antibodies which specifically bind to SEQ ID NO:2, a human variant of SEQ ID NO:2 (note that the protein target in Blake was a mouse protein, as well having only 17% amino acid homology to SEQ ID NO:2), or a fragment of at least 10 amino acids of SEQ ID NO:2. Paul contains teachings on the superiority of polyclonal antibodies for particular purposes, but has no disclosure of antibodies that bind to any proteins related to SCAH-2; thus it does not make up for the deficiencies of Blake et al.

Claims 1, 2, 6-8, and 14 are also rejected under 35 U.S.C. § 103(a) as allegedly being obvious over Blake et al. in view of Thorpe and Kerr. Claims 1, 2, and 6-11 are rejected under 35 U.S.C. § 103(a) as allegedly being obvious over Blake et al, in view of Schlom. As discussed above, Blake et al. does not anticipate the claimed monoclonal antibodies. Neither Thorpe and Kerr, which

teaches methods of labeling antibodies, nor Schlom, which teaches the advantages of Fab antibodies, and the preparation of Fab fragments from recombinant immunoglobulin libraries, makes up for the deficiencies of Blake et al.

Claims 1-9 and 14 are rejected under 35 U.S.C. § 103(a) as allegedly being obvious over Reiter et al. in view of Schlom. As discussed above, Reiter et al. is not prior art to the claimed invention, thus it has no bearing on a determination as to what would be obvious before the filing of the instant application.

Withdrawal of the rejections under 35 U.S.C. § 103 is therefore respectfully requested.

CONCLUSION

In light of the above amendments and remarks, Applicants submit that the present application is fully in condition for allowance, and request that the Examiner withdraw the outstanding objections/rejections. Early notice to that effect is earnestly solicited.

If the Examiner contemplates other action, or if a telephone conference would expedite allowance of the claims, Applicants invite the Examiner to contact the undersigned at the number listed below.

Applicants believe that no fee is due with this communication. However, if the USPTO determines that a fee is due, the Commissioner is hereby authorized to charge Deposit Account No. **09-0108**.

Respectfully submitted,

INCYTE CORPORATION

Date: December 12, 2003

Barrie Greene

Barrie D. Greene

Reg. No. 46,740

Direct Dial Telephone: (650) 621-7576

Customer No.: 27904
3160 Porter Drive
Palo Alto, California 94304
Phone: (650) 855-0555
Fax: (650) 849-8886

Attachments:

1. Kimball, J.W., *Introduction to Immunology*, 2nd Ed., Macmillan Publishing Company, New York, 1986
2. Saffran, D.C. et al., "Anti-PSCA mAbs inhibit tumor growth and metastasis formation and prolong the survival of mice bearing human prostate cancer xenografts" *Proc. Natl. Acad. Sci. USA* (2001) 98:2658-2663
3. Amara, N. et al., "Prostate stem cell antigen is overexpressed in human transitional cell carcinoma" *Cancer Res.* (2001) 61:4660-4665

4. Ross, S. et al., "Prostate stem cell antigen as therapy target: Tissue expression and in vivo efficacy of a immunoconjugate" Cancer Res. (2002) 62:2546-2553
5. Exhibit A: ClustalW sequence alignment of SCAH-2 with mouse Ly-6A.2/E.1

This Page Is Inserted by IFW Operations
and is not a part of the Official Record

BEST AVAILABLE IMAGES

Defective images within this document are accurate representations of the original documents submitted by the applicant.

Defects in the images may include (but are not limited to):

- BLACK BORDERS
- TEXT CUT OFF AT TOP, BOTTOM OR SIDES
- FADED TEXT
- ILLEGIBLE TEXT
- SKEWED/SLANTED IMAGES
- COLORED PHOTOS
- BLACK OR VERY BLACK AND WHITE DARK PHOTOS
- GRAY SCALE DOCUMENTS

IMAGES ARE BEST AVAILABLE COPY.

As rescanning documents *will not* correct images,
please do not report the images to the
Image Problem Mailbox.

Introduction to Immunology

SECOND EDITION

John W. Kimball

Macmillan Publishing Company
New York
Collier Macmillan Publishers
London

To
A. M. Pappenheimer, Jr.
Professor of Biology *Emeritus*, Harvard University

Copyright © 1986, Macmillan Publishing Company, a division of Macmillan, Inc.
Printed in the United States of America

All rights reserved. No part of this book may be reproduced or
transmitted in any form or by any means, electronic or mechanical,
including photocopying, recording, or any information storage and
retrieval system, without permission in writing from the publisher.

Earlier edition copyright © 1983 by Macmillan Publishing Company

Macmillan Publishing Company
866 Third Avenue, New York, New York 10022
Collier Macmillan Canada, Inc.

Library of Congress Cataloging in Publication Data

Kimball, John W.

Introduction to immunology.

Includes bibliographies and index.

1. Immunology. I. Title. [DNLM: 1. Immunity.]

QW 504 K49i]

QR181.K49 1986

616.07'9

85-10607

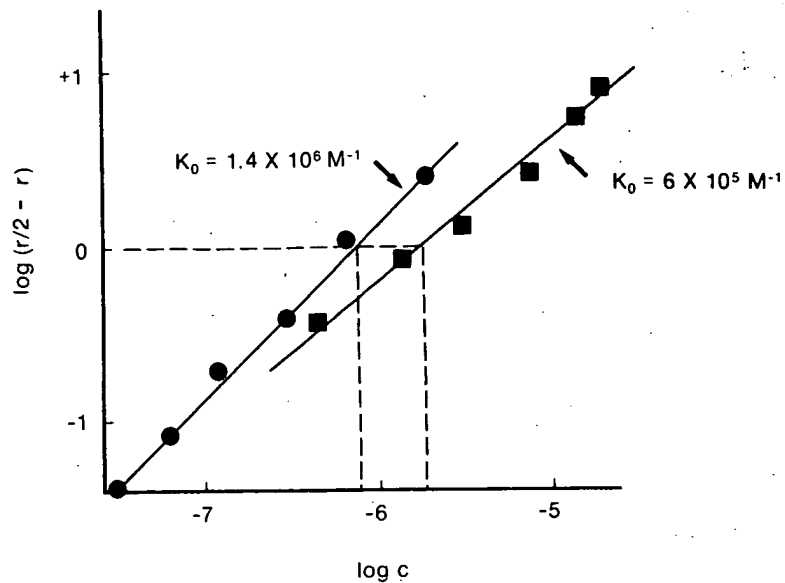
ISBN 0-02-363830-3

Printing: 4 5 6 7 8 Year: 7 8 9 0 1 2 3 4 5

ISBN 0-02-363830-3

tchard plot of the 4.10. Although this bodies was heterogeneous to its affinity for the fine an average nt, K_0 , which is the concentration of free one-half of all the illed ($r = 1$). In this 10^5 M^{-1} .

Figure 4.12 Sips plot of the results given in Figure 4.8 (upper line) and 4.10 (lower line). The slope of the upper line is 1, showing homogeneous binding. The slope of the lower line is 0.8, showing that this population of antibody molecules is heterogeneous with respect to its affinity for the ligand. The value of the slope, a , is called the heterogeneity index.



antibodies discussed

concentration of free tly from a Scatchard tiserum represented

is vary over a consid- bie determinants like M^{-1} and occasionally end of the range for dependent upon ionic Antipolysaccharide

slotted in Figure 4.9 equation.

c

straight line (Figure ectly from the plot. ne reciprocal of that 2).

neity index. It repre- ality of antibodies , and the slope of the enting a spectrum of d antipneumococcal

antiserum, which we have already seen is heterogeneous with respect to affinity, has a heterogeneity index of 0.8 (and the slope of its Sips plot is likewise 0.8).

If we are justified in assuming that the dispersion of individual K values in the population of antibody molecules is distributed symmetrically around K_0 , then the coefficient a becomes a measure of the breadth of the resulting bell-shaped curve. For the example given ($a = 0.8$), roughly 75% of the antibody molecules in the preparation have affinities between 1.6×10^5 and $2.2 \times 10^6 \text{ M}^{-1}$.

In many, perhaps most, antisera, there are good reasons to believe that the distribution of affinities does *not* follow a normal statistical distribution, i.e., would not yield a bell-shaped curve. Despite this, Sips plots remain a useful way of comparing different antibody preparations with respect to their average affinities and—subject to the qualification mentioned—their relative heterogeneity of affinities.

4.5 The Specificity of Antibodies

The specificity of an antibody molecule is its ability to discriminate between the antigenic determinant against which it was elicited and other antigenic determinants of related structure. The antigenic determinant, for example, a hapten like the dinitrophenyl group (DNP), present on the immunogen is called the *homologous determinant*; related structures (e.g., the trinitrophenyl group, TNP) are said to be *heterologous*.

The ability of an antibody molecule to discriminate between homologous and heterologous determinants can be detected by any assay that measures the binding between the two. If the antibody reacts measurably with a heterologous determinant, it is said to show a cross reaction.

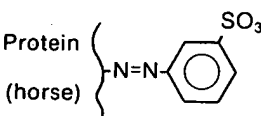
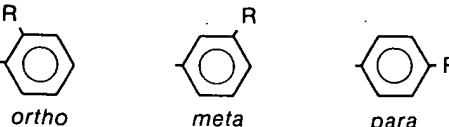
IMMUNOGEN:			
HAPTENS OF TEST ANTIGENS:			
$R = SO_3^-$	\pm	$++\pm$	\pm
$R = AsO_3H^-$	0	+	0
$R = COO^-$	0	\pm	0

Figure 4.13 Antibody specificity. Relative amounts of precipitation of rabbit antibodies directed against the homologous hapten (*m*-azobenzenesulfonate) and a variety of heterologous haptens. The antibodies were elicited by immunizing with the homologous hapten coupled to horse serum proteins. The tests were performed with all the haptens coupled to chicken serum proteins thus restricting the reaction to antibodies directed against the haptens. [From K. Landsteiner, *The Specificity of Serological Reactions*, 2nd ed., reprinted by Dover Publications, New York, 1962.]

The earliest systematic studies of antibody specificity were carried out by Karl Landsteiner and his colleagues. They used precipitation in liquid as a semiquantitative assay with which to compare homologous and heterologous reactions. In one series of experiments, antibodies were elicited (in rabbits) to a mixture of horse serum proteins that had been conjugated with the hapten *m*-azobenzenesulfonate (Figure 4.13). The resulting antisera were tested for reactivity with chicken serum proteins that had been conjugated with (1) the same hapten or (2) haptens in which the sulfonate group was in the ortho or para position or (3) azobenzenearsonate or azobenzenecarboxylate, in each case either ortho, meta, or para. The results are shown in Figure 4.13. As you can see, the antibodies reacted with the homologous hapten on the new carrier proteins (as we would predict from the discussion in Section 1.4). The most copious precipitate was formed when the sulfonate group was located in the meta (the homologous) position, although measurable precipitation occurred when its position was either ortho or para. Neither azobenzenearsonate nor azobenzenecarboxylate produced any precipitation except when the charged group was present in the meta position. So, while these antibodies do show cross-reactivity, the reduced reaction with heterologous ligands reveals a substantial degree of specificity.

Equilibrium dialysis provides a method by which antibody specificity can be assessed in a more quantitative manner. With this procedure, a value for K_0 can be determined for the homologous ligand as well as for related ligands. The greater the difference between the K_0 for the homologous ligand and that for a heterologous ligand, the greater the specificity of the antibody molecule for the homologous ligand. The data in Figure 4.14 show the results of equilibrium dialysis performed on a population of antibodies elicited by a protein carrying DNP groups covalently bound to the epsilon amino groups of lysine residues. As is generally the case, these antibodies had the highest K_0 for the homologous ligand (ϵ -DNP-*L*-lysine). However, they also displayed substantial affinity for related ligands, even to dinitrobenzene itself. On occasions, an antigen will elicit antibodies that bind *more* strongly to a heterologous

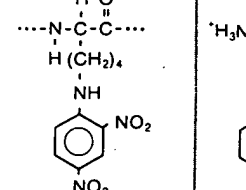
IMMUNOGEN	
	ϵ -DNI

Figure 4.14 Antibody specificity. Rabbit antibodies were immunized with ϵ -DNP-*L*-lysine coupled to the ϵ -amino groups of the β -chain of bovine gamma globulin (DNP-BGG). The antibodies were then tested for their affinity for ϵ -DNI, which has one less DNP group than the immunogen. The affinity constant, K_0 , was determined by equilibrium dialysis. [From W. M. Huggins, in "Radioimmunoassay," *Handbook of Experimental Immunology*, 3rd ed., D. M. Weir (ed.), Blackwell, Boston, 1978.]

Figure 4.15 The specificity of antibodies elicited by a protein carrying DNP groups. The figure shows a graph of the ratio of binding to homologous ligand to binding to heterologous ligand (B_h/B_h) versus the concentration of the heterologous ligand (M). The curve shows a sharp increase in the ratio as the concentration of the heterologous ligand increases, indicating a 1000-fold increase in affinity for the homologous ligand. The data points are as follows:

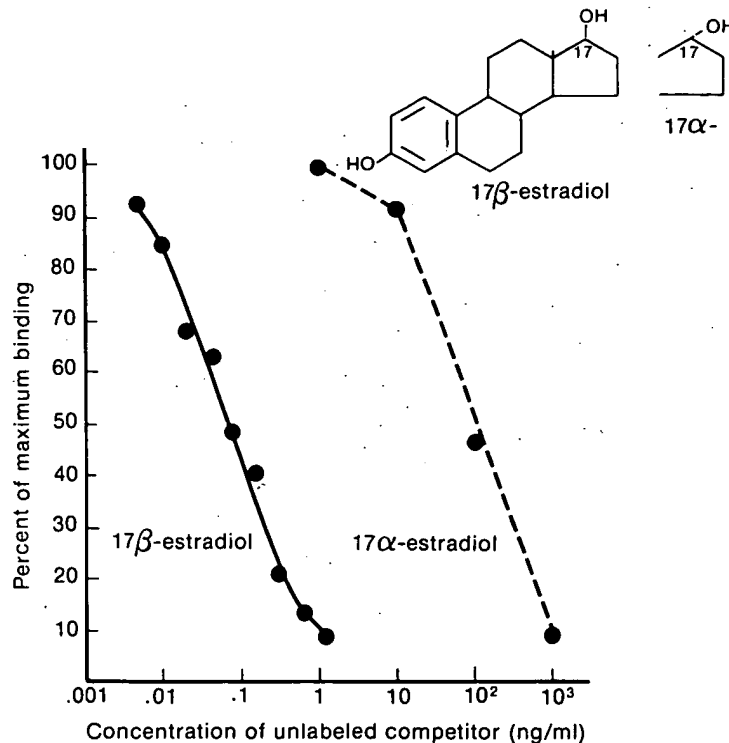
Concentration of heterologous ligand (M)	B _h /B _h
0.001	1.0
0.01	1.0
0.1	1.0
1.0	1.0
10.0	1.0
100.0	1.0
1000.0	1000.0

IMMUNOGEN	HAPTENS			
H O ---N---C---C--- $\text{H} (\text{CH}_2)_4$ NH 	H $^*\text{H}_3\text{N---C---COO}^-$ $(\text{CH}_2)_4$ NH 	H $^*\text{H}_3\text{N---C---COO}^-$ $(\text{CH}_2)_3$ NH 		
DNP-BGG	ϵ -DNP-lysine	δ -DNP-ornithine	2,4-dinitroaniline	<i>m</i> -dinitrobenzene

Figure 4.14 Antibody specificity revealed by equilibrium dialysis. A rabbit was immunized with a hapten–carrier conjugate consisting of DNP groups coupled to the ϵ -amino groups of the lysine residues of bovine gamma globulin (DNP–BGG). The resulting antiserum had an affinity for ϵ -DNP-lysine of $2.3 \times 10^7 \text{ M}^{-1}$ but less than half that affinity for δ -DNP-ornithine which has one less carbon atom in the chain. The degree to which an antibody population discriminates between the homologous and heterologous ligands is a measure of the specificity of that population. [From H. N. Eisen and G. W. Siskind, *Biochemistry* 3:996, 1964.]

y were carried out precipitation in liquid homologous and heterologous antibodies were elicited in animals that had been immunized (Figure 4.13). The antigenic serum proteins may be (1) proteins or (2) haptens in their position or (3) azo-casein either ortho, meta, or para. As you can see, the new carrier protein (Figure 1.4). The most prominent precipitin loop was located in the middle of the double precipitation either azobenzene or azobisisobutyronitrile precipitation experiment. So, while the reaction with the hapten showed specificity, the antibody specificity was not as good as for the homologous antigen. The data in Figure 4.13 was performed on a rabbit that had been immunized with DNP groups covalently linked to bovine albumin. As is generally the case, the homologous reaction showed substantial affinity. On occasions, an antibody can react with a heterologous antigen.

Figure 4.15 The shift of the hydroxyl group on carbon 17 from the beta position (extending above the plane of the molecule) to the alpha position (extending below) lowers by 1000-fold the affinity of the molecule for antibodies raised against a 17β -estradiol-BSA conjugate. In each case the binding was measured by radioimmunoassay (see Section 5.9). [From W. M. Hunter, "Radioimmunoassay" in *Handbook of Experimental Immunology*, 3rd ed., Vol. 1, D. M. Weir (ed.), Blackwell, 1978.]



determinant than to the homologous determinant. Such antibodies are said to be *heteroclitic*.

The specificity of antibodies extends to their being able to discriminate between stereoisomers of the same molecule. 17β -Estradiol is the major estrogen found in women of reproductive age. Antibodies elicited by a 17β -estradiol-BSA conjugate bind strongly to the homologous hapten. When presented with 17α -estradiol, however, the binding efficiency is reduced over 1000-fold (Figure 4.15). The single change in the orientation of the hydroxyl group at carbon 17 from the beta configuration (projecting above the plane of the molecule) to the alpha configuration (projecting below the plane) is responsible for this sharp drop in affinity.

4.6 The Specificity of Antisera

The concept of specificity as applied to individual antibody molecules differs somewhat from the concept as applied to antisera. Most antisera represent complex mixtures of antibody molecules. These antisera usually display many specificities. This multispecificity arises in two ways.

1. If an animal is immunized with two or more different antigens, the resulting antiserum will react independently with each. Thus Landsteiner's rabbits produced not only anti-azobenzenearsonate antibodies but also antibodies against the many different proteins present in horse serum (which is why he had to use substituted chicken proteins for his assays of antihapten activity).

An antiserum that is specific for a single antigen can be produced in several ways. One is to immunize the animal with a preparation of the antigen that has been sufficiently purified so that no contaminating molecules remain in immunogenic concentrations. For example, we can produce a rabbit antiserum specific for human albumin by immunizing the rabbit with the purified protein rather than with whole human serum.

2. Often the problems of multispecificity cannot be solved simply by immunizing with pure antigen. For example, an antiserum raised against purified human IgG will also react with human IgA and IgM because each of the classes of immunoglobulin uses the same light chains (κ and λ). However, this antiserum can be made specific for IgG by exposing it to an appropriate immunoabsorbent: particles to which other molecules containing the light chains (e.g., IgA or IgM) have been attached. Those antibodies directed against determinants on the light chains will bind to the immunoabsorbent and can be removed from the antiserum. The antibodies that remain will now be specific for IgG, i.e., specific for its heavy (γ) chains. So even if we produce an antiserum that is specific for a single antigen molecule (i.e., human albumin), this specificity is still only relative. Most antigens display several different antigenic determinants, each of which can elicit the formation of a population of antibodies directed against it. Thus an antigen bearing determinants A, B, C, and D will give rise to four separate sets of antibodies, each set directed against one of the determinants. When such an antiserum is presented to an

antigen displaying so ample, A and C, the precipitate the mole kind: the interaction cause of certain deter

4.7 Purification o

In the preceding secti remove cross-reactin were interested in wh a tool of great genera specificity.

The procedure inv

Step 1. The immu (e.g., DNP) to a solid or other polymers ca

Step 2. The antis 4.16). As long as the antibodies in the mix tained. Antibodies of pass through unimp

Step 3. Elution. A antibodies from the i centration of salts and lent interactions bet agent, such as 8 M u configuration of the a to elute with a soluble DNP-lysine run into bent for the antigen antibodies to the fluid

Step 4. Dialysis. I buffered saline in ord

The result of this pi is a preparation of a preparation is "pure" means pure with res contained in it. Elec mally reveal as broad

Anti-PSCA mAbs inhibit tumor growth and metastasis formation and prolong the survival of mice bearing human prostate cancer xenografts

Douglas C. Saffran*, Arthur B. Raitano*, Rene S. Hubert*, Owen N. Witte†‡, Robert E. Reiter§, and Aya Jakobovits*†

*UroGenesys, Inc., 1701 Colorado Avenue, Santa Monica, CA 90404; and Departments of †Microbiology, Immunology, and Molecular Genetics,

‡Howard Hughes Medical Institute, and §Department of Urology, University of California, Los Angeles, CA 90095

Contributed by Owen N. Witte, December 28, 2000

Prostate stem-cell antigen (PSCA) is a cell-surface antigen expressed in normal prostate and overexpressed in prostate cancer tissues. PSCA expression is detected in over 80% of patients with local disease, and elevated levels of PSCA are correlated with increased tumor stage, grade, and androgen independence, including high expression in bone metastases. We evaluated the therapeutic efficacy of anti-PSCA mAbs in human prostate cancer xenograft mouse models by using the androgen-dependent LAPC-9 xenograft and the androgen-independent recombinant cell line PC3-PSCA. Two different anti-PSCA mAbs, 1G8 (IgG1κ) and 3C5 (IgG2aκ), inhibited formation of s.c. and orthotopic xenograft tumors in a dose-dependent manner. Furthermore, administration of anti-PSCA mAbs led to retardation of established orthotopic tumor growth and inhibition of metastasis to distant sites, resulting in a significant prolongation in the survival of tumor-bearing mice. These studies suggest PSCA as an attractive target for immunotherapy and demonstrate the therapeutic potential of anti-PSCA mAbs for the treatment of local and metastatic prostate cancer.

Prostate cancer is the most commonly diagnosed cancer and is the second leading cause of cancer-related deaths in American males (1). Despite curative therapies for localized disease such as radical prostatectomy, radiation therapy, and cryotherapy, approximately one-third of treated patients will relapse (2, 3). Androgen-ablation therapy is effective initially in advanced metastatic disease, but in most cases androgen-independent tumors develop for which there is no available effective therapy (3). Recently, mAb therapy has proven efficacious in clinical cancer treatment, including an anti-CD20 mAb (Rituxan) for B cell lymphoma (4) and an anti-Her2/neu mAb (Herceptin) for metastatic breast cancer (5). Development of antibody therapeutics for prostate cancer is limited by the paucity of cell-surface antigens expressed at a high frequency and at a significant level in prostate-cancer patients and with a restricted expression pattern in normal tissues. At present, antibodies to only one such target antigen, prostate-specific membrane antigen, are being developed toward clinical trials (6, 7).

Recently, we reported the identification and characterization of prostate stem-cell antigen (PSCA), a cell-surface antigen that is predominantly prostate specific and expressed in the majority of prostate-cancer patients (8–10). PSCA is a glycosylphosphatidylinositol-anchored 123-aa protein related to the Ly-6 family of cell-surface proteins. *In situ* hybridization and immunohistochemical (IHC) analysis demonstrated PSCA expression in over 80% of local disease specimens and in all bone metastatic lesions examined (8, 9). Elevated PSCA expression was shown to correlate with increased tumor stage, grade, and progression to androgen independence (9). The significant cell-surface expression of PSCA in localized and advanced disease, together with its restrictive expression in normal tissues (9), makes PSCA a potential target for immunotherapy. Recent studies have indicated PSCA to be a target for T cell-based immunotherapy (11);

however, PSCA antibody therapy has not been investigated yet.

Here we examined the anti-tumor efficacy of two anti-PSCA mAbs with different isotypes and affinities: 1G8 (IgG1κ; $K_D = 10^{-9}$ M) and 3C5 (IgG2aκ; $K_D = 4.3 \times 10^{-8}$ M). Antibody efficacy on tumor growth and metastasis formation was studied primarily in a mouse orthotopic prostate-cancer xenograft model. In this report we demonstrate that anti-PSCA mAbs are able to inhibit formation of both the androgen-dependent LAPC-9 (12) and the androgen-independent PC3-PSCA (13) tumor xenografts. Anti-PSCA mAbs also retarded the growth of established orthotopic tumors significantly and prolonged survival of tumor-bearing mice. Strikingly, antibody treatment resulted in nearly a complete inhibition of lung metastasis formation in tumor-bearing mice. These results indicate the potential utility of anti-PSCA mAbs in the treatment of local and advanced stages of prostate cancer.

Materials and Methods

Prostate Cancer Xenografts and Cell Lines. The LAPC-9 xenograft, which expresses a wild-type androgen receptor and produces prostate-specific antigen (PSA), was passaged in 6- to 8-week-old male ICR-severe combined immunodeficient (SCID) mice (Taconic Farms) by s.c. trocar implant (12). Single-cell suspensions of LAPC-9 tumor cells were prepared as described (12). The prostate carcinoma cell line PC3 (American Type Culture Collection) was maintained in DMEM supplemented with L-glutamine and 10% (vol/vol) FBS. A PC3-PSCA cell population was generated by retroviral gene transfer as described (14). Expression of PSCA on the cell surface was determined by staining 1×10^6 cells at 4°C for 30 min with 1 μg of either the 1G8 or 3C5 mAbs and 1 μg of IgG1 or IgG2a isotype control antibodies, respectively. Anti-PSCA staining was detected by using an FITC-conjugated goat anti-mouse antibody (Southern Biotechnology Associates) followed by analysis on a Coulter Epics-XL flow cytometer.

Purification and Characterization of Anti-PSCA mAbs. The 1G8 (IgG1κ) and 3C5 (IgG2aκ) anti-PSCA hybridomas, derived from mice immunized with a glutathione S-transferase-PSCA fusion protein (9), were purified from ascites. Affinity measurements were performed by surface plasmon resonance technology using BIAcore 2000 (Amersham Pharmacia) with purified mAbs and purified secPSCA immobilized at low density (30 RU). The association- and dissociation-rate constants were determined by using CLAMP software (15).

Abbreviations: PSCA, prostate stem-cell antigen; IHC, immunohistochemical; PSA, prostate-specific antigen; SCID, severe combined immunodeficient; STEAP, six-transmembrane epithelial antigen of the prostate.

*To whom reprint requests should be addressed. E-mail: ajakobovits@urogenesys.com.

The publication costs of this article were defrayed in part by page charge payment. This article must therefore be hereby marked "advertisement" in accordance with 18 U.S.C. §1734 solely to indicate this fact.

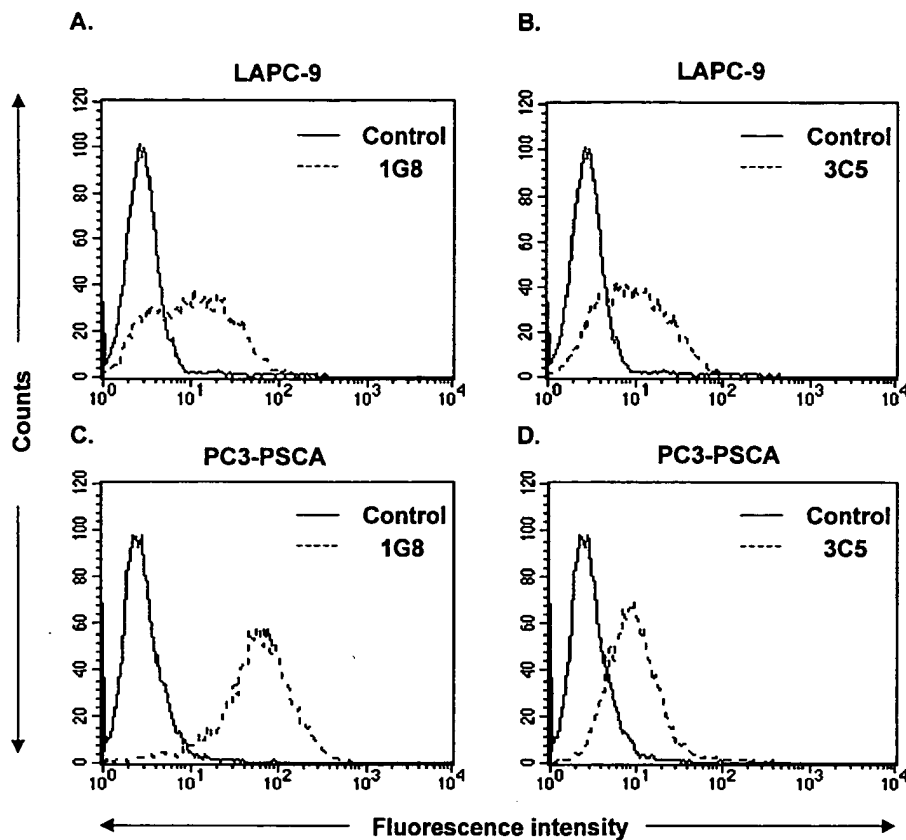


Fig. 1. Detection of cell-surface PSCA expression by anti-PSCA mAbs using flow cytometry. (A and B) LAPC-9 cells were stained with either 1G8 (A) or 3C5 (B) mAbs (dotted line) and the corresponding isotype control antibodies (solid line) IgG1 (A) or IgG2a (B). (C and D) PC3-PSCA cells were stained with either 1G8 (C) or 3C5 (D) mAbs (dotted line). As a control, PC3 cells (solid line) were stained with 1G8 (C) or 3C5 (D).

Xenograft Mouse Models. S.c. tumors were generated by injection of 1×10^6 LAPC-9, PC3, or PC3-PSCA cells mixed at a 1:1 dilution with Matrigel (Collaborative Research) in the right flank of male SCID mice. To test antibody efficacy on tumor formation, i.p. antibody injections started on the same day as tumor-cell injections. As a control, mice were injected with either purified mouse IgG (ICN) or PBS. In preliminary studies, we found no difference between mouse IgG or PBS on tumor growth. Tumor sizes were determined by vernier caliper measurements, and the tumor volume was calculated as length \times width \times height. Mice with s.c. tumors greater than 1.5 cm in diameter were killed in accordance with University of California Los Angeles Animal Rights Committee guidelines. PSA levels were determined by using a PSA ELISA kit (Anogen, Mississauga, Ontario). Circulating levels of 3C5 or 1G8 mAbs were determined by a capture ELISA kit (Bethyl Laboratories, Montgomery, TX). Antibody half-life in SCID mice was determined to be 14–15 days.

Orthotopic injections were performed under anesthesia by using ketamine/xylazine. An incision was made through the abdominal muscles to expose the bladder and seminal vesicles, which then were delivered through the incision to expose the dorsal prostate. LAPC-9 cells (5×10^5) mixed with Matrigel were injected into each dorsal lobe in a 10- μ l volume. To monitor tumor growth, mice were bled on a weekly basis for determination of PSA levels. Based on the PSA levels, the mice were segregated into groups for the appropriate treatments. To test the effect of anti-PSCA mAbs on established orthotopic tumors, i.p. antibody injections started when PSA levels reached 2–80 ng/ml.

IHC Analysis of Tissue Specimens. IHC analysis was performed on 4- μ m formalin-fixed paraffin-embedded prostate and lung tissues derived from mice bearing orthotopic LAPC-9 tumors. Then 50 serial sections were cut from each lung, and every 10th section was stained for expression of the prostate-specific marker six-transmembrane epithelial antigen of the prostate (STEAP) by using an anti-STEAP polyclonal antibody (14). Micrometastases consisting of at least two visible cells in a crosssectional view were scored as positive.

Statistical Analysis. Mean tumor volumes and PSA levels were compared between groups by using a Mann–Whitney *U* test. *P* values <0.05 were considered significant statistically. Mouse survival was analyzed by using a log rank test. *P* values <0.05 were considered significant statistically.

Results and Discussion

Two anti-PSCA mAbs, 1G8 (IgG1 κ) and 3C5 (IgG2a κ), were analyzed for anti-tumor activity on the androgen-dependent LAPC-9 xenograft and androgen-independent PC3 cell line engineered to express PSCA (PC3-PSCA), both derived from bone metastases from patients with advanced prostate cancer (12, 13). Flow-cytometric analysis confirmed the ability of anti-PSCA mAbs to detect expression of native PSCA protein on the surface of LAPC-9 and PC3-PSCA cells (Fig. 1). Antibody binding was shown to lead to antigen internalization (data not shown). The 1G8 and 3C5 mAbs were shown previously to recognize the middle portion (amino acids 46–85) and the amino-terminal portion (amino acids 21–50) of the PSCA extracellular domain, respectively (9). Affinities of 1G8 and 3C5 mAbs were determined to be 1×10^{-9} M ($K_{on} = 1.68 \times 10^5$; K_{off}

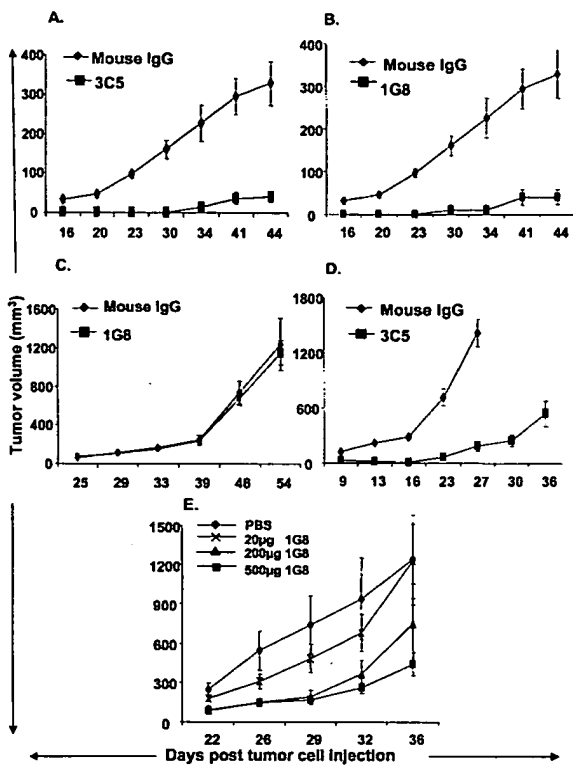


Fig. 2. Inhibition of s.c. tumor formation by anti-PSCA mAbs. (A–E). Male SCID mice were injected s.c. with 1×10^6 PC3-PSCA (A and B), PC3 (C), or LAPC-9 (D and E) cells in conjunction with i.p. injection of either 200 µg of 3C5 (A and D) or 1G8 (B and C) mAb (■) or 200 µg control mouse IgG (A–D, ♦). Antibody doses administered in E were either 20 (×), 200 (▲), or 500 µg (■), and PBS (◆) was used as a control. All treatments were carried out three times a week for 2 weeks (six injections total) on eight mice in each group. The data are presented as mean tumor volume (mm^3) \pm SEM.

$= 1.69 \times 10^{-4}$) and 4.3×10^{-8} M ($K_{\text{on}} = 8.3 \times 10^3$; $K_{\text{off}} = 3.58 \times 10^{-4}$), respectively, by solid-phase measurements using purified PSCA extracellular domain as the antigen.

Anti-PSCA mAbs Inhibit Formation of PSCA-Expressing Prostate-Cancer Tumors. To determine whether the anti-PSCA mAbs could inhibit formation of PSCA-expressing tumors *in vivo*, we performed a series of experiments by using 1G8 and 3C5 mAbs with both LAPC-9 and PC3-PSCA xenograft tumors. In the first series of experiments, tumor cells were injected s.c. in the flanks of male SCID mice in conjunction with i.p. injection of 200 µg of 1G8 or 3C5 mAbs or control mouse IgG. Antibody was administered three times per week for two consecutive weeks. Treatment with either 1G8 or 3C5 mAb inhibited formation of PC3-PSCA tumors compared with mice treated with control antibody (Fig. 2 A and B). Tumor growth was suppressed completely in both the 1G8- and 3C5-treated groups ($P = 0.002$ and $P < 0.001$, respectively) until 14 days after the last antibody injection, at which point tumors grew but at a significantly reduced rate. At day 44 (28 days after last antibody injection), tumor sizes were approximately 8-fold lower in both the 1G8- and 3C5-treated groups (41 mm^3) as compared with the control group (328 mm^3). The 1G8 mAb had no effect on the formation of tumors from parental PC3 cells that do not express PSCA (Fig. 2C), demonstrating that the effect on tumor growth results from specific binding to PSCA.

Inhibition of s.c. tumor formation also was observed by antibody treatment of LAPC-9 tumors. LAPC-9 xenografts, which were propagated *in vivo* since their establishment from

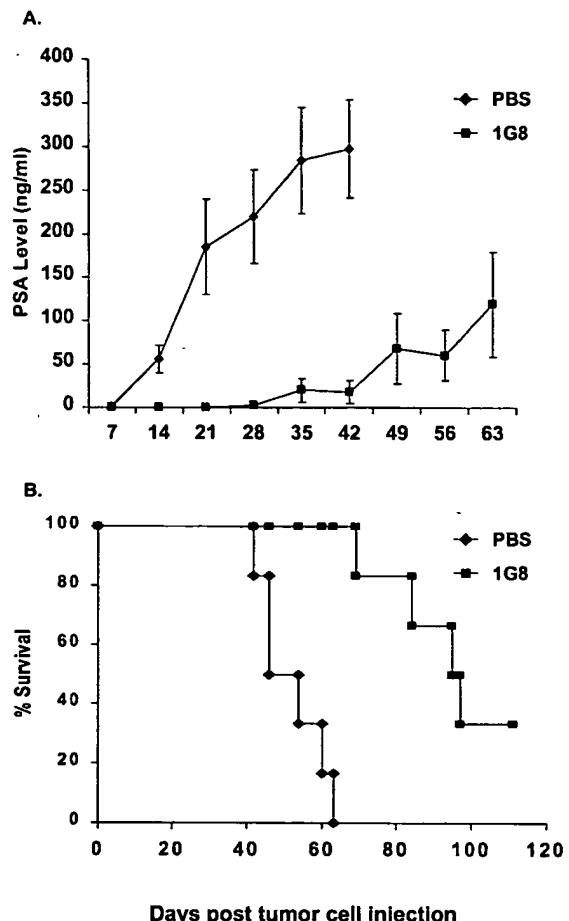


Fig. 3. Inhibition of orthotopic tumor formation by anti-PSCA mAb. LAPC-9 (5×10^5) cells were injected into each dorsal lobe of the prostate in male SCID mice. After 2 days, mice ($n = 6$) were injected i.p. with 200 µg of 1G8 (■) or PBS (♦) three times per week for 2 weeks. (A) Tumor growth was monitored by measuring PSA levels on the indicated days. Each data point represents the mean serum PSA levels (\pm SEM) for each group of six mice. (B) Significant prolongation of survival of mice treated with 1G8 (■) compared with mice treated with PBS (♦). The percentage of survival is shown for each group at the indicated time points.

patient-derived bone metastasis, exhibit more aggressive growth than PC3-PSCA (Fig. 2 D and E). Administration of 3C5 to LAPC-9-injected mice (six injections of 200 µg) resulted in complete inhibition of tumor formation until day 16, as compared with control mice, with a significant reduction ($P < 0.001$) in tumor-growth rate afterward (Fig. 2D). At day 27, 11 days after the last antibody injection, tumors in the 3C5-treated mice reached a mean size of 190 mm^3 , whereas the mice in the control group exhibited a mean size of $1,400 \text{ mm}^3$ and had to be killed. At day 26, the PSA levels in 3C5-treated mice were 2 ng/ml as compared with 80 ng/ml in the control group, providing further evidence for the antibody effect on tumor formation. Initiation of tumor growth correlated with 2-fold decrease in circulating 3C5 antibody levels (data not shown).

Antibody dose-response experiments were carried out by injecting LAPC-9 cells into mice concomitantly with doses of 20, 200, or 500 µg 1G8 mAb or PBS as a control. Antibody treatment was performed three times per week for two consecutive weeks and resulted in inhibition of LAPC-9 tumor growth in a dose-dependent manner (Fig. 2E). Both the 200- and 500-µg doses demonstrated equivalent and significant ($P < 0.01$) inhibition of tumor growth up to day 29, 17 days after the last antibody

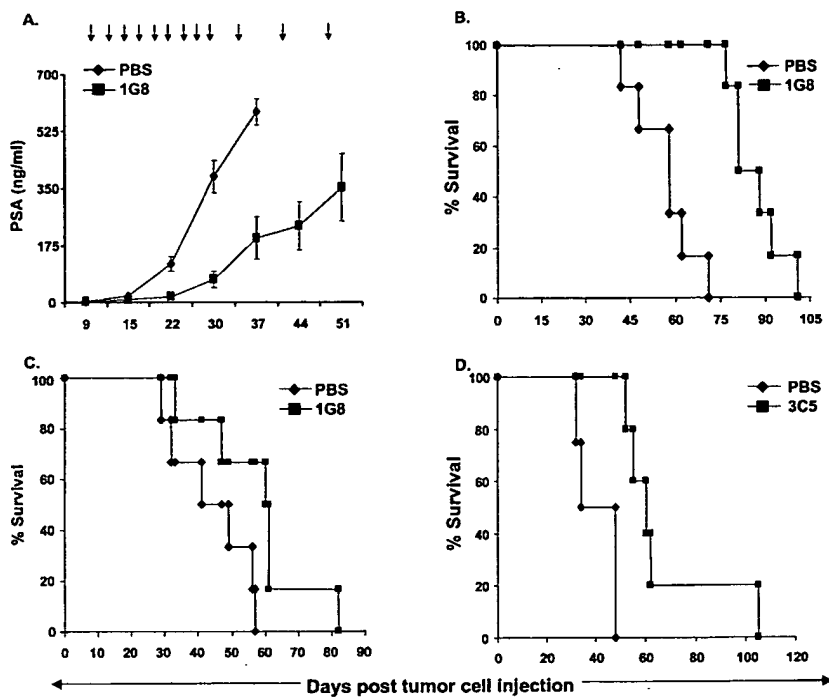


Fig. 4. Growth retardation of established LAPC-9 orthotopic tumors and prolongation of survival of tumor-bearing mice by anti-PSCA mAbs. (A) Mice ($n = 6$) with PSA levels of 2–3 ng/ml (day 9) were treated with either PBS (◊) or 2 mg 1G8 (■) three times for 1 week followed by nine injections of 1 mg during the next 3 weeks, as indicated by arrows. Tumor growth was monitored by measuring serum PSA levels, and each data point represents the mean PSA level (\pm SEM). (B) Significant prolongation of survival of 1G8-treated mice (■) in A compared with PBS control mice (◊). The percentage of survival is shown for each group at the indicated time points. (C) Mice ($n = 5$) with PSA levels of 64–78 ng/ml (day 13) were given 10 injections of 1 mg of 1G8 for 4 weeks. The percentage of survival is shown for each group at the indicated time points. (D) Mice ($n = 6$) with PSA levels 14–16 ng/ml (day 7) were injected with 2 mg of 3C5 three times for 1 week, followed by seven injections of 1 mg 3C5 mAb for the next 3 weeks. The percentage of survival is shown for each group at the indicated time points.

injection. Increased tumor volumes were detected in those mice at day 32, at which point a difference in efficacy between the 200- and 500- μ g doses became apparent. Minimal inhibition of tumor growth was detected in the group of mice treated with 20 μ g 1G8 mAb. The effect of mAb on tumor volumes was corroborated by a dose-dependent reduction in PSA levels detected in 1G8-treated mice (data not shown).

We next tested the effect of anti-PSCA mAbs on tumor formation by using the LAPC-9 orthotopic model. As compared with the s.c. model for tumor growth, the orthotopic model, which requires injection of tumor cells directly in the mouse prostate, results in local tumor growth, development of metastasis in distal sites, deterioration of mouse health, and subsequent death (16, 17). These features make the orthotopic model more representative of human disease progression and allowed us to follow the therapeutic effect of mAbs on clinically relevant end points. LAPC-9 tumor cells were injected into the mouse prostate, and 2 days later the mice were segregated into two groups and treated with either 200 μ g of 1G8 mAb or PBS three times per week for two weeks. Mice were monitored weekly for circulating PSA levels as an indicator of tumor growth. In the PBS control group, PSA levels rose steadily to reach mean PSA levels of over 200 ng/ml by day 28 (Fig. 3A). No detectable PSA levels were observed in the 1G8-treated mice up to day 28, 12 days after the last antibody injection, suggesting a complete inhibition of LAPC-9 tumor growth. PSA levels started to be detectable in the serum of 1G8-treated mice 19 days after the last antibody injection, likely as a result of the significant drop in 1G8 serum concentration (over 3-fold reduction from day-16 levels, data not shown). At all time points, PSA levels in the 1G8-treated mice were significantly lower as compared with the PBS-control mice ($P < 0.002$). Survival of 1G8-treated mice was

also prolonged significantly ($P = 0.0005$). All untreated mice died within 42–63 days, whereas 50% of 1G8-treated mice were still alive by day 95 (Fig. 3B). Together, these results demonstrate the ability of anti-PSCA mAbs to inhibit tumor formation in both s.c. and orthotopic tumor models. In both tumor models, initiation of tumor growth paralleled a significant drop in the concentration of serum anti-PSCA antibodies. Animals treated with anti-PSCA mAbs showed a significantly reduced tumor-growth rate as compared with untreated mice.

Anti-PSCA mAbs Retard the Growth of Established Orthotopic Tumors and Prolong Survival of Tumor-Bearing Mice. Orthotopic injection of LAPC-9 cells results in aggressive local tumor growth and metastasis, leading to deteriorated health and eventual death within 6–7 weeks (Fig. 3). This feature allowed us to study the effect of the anti-PSCA mAbs not only on tumor growth but also the health and survival of mice bearing orthotopic LAPC-9 tumors. Initially, we studied the effect of the 1G8 mAb in mice with low established tumor burden (PSA levels 2–3 ng/ml). Mice were injected three times with 2 mg of 1G8 mAb during the first week, followed by nine injections of 1 mg over a 4-week period. A control group was injected with PBS. Tumor growth was monitored weekly by measuring serum PSA levels in both groups. Treatment of the LAPC-9 tumor-bearing mice with 1G8 mAb resulted in highly reduced PSA levels as compared with the control group, demonstrating significant ($P = 0.002$) inhibition of tumor growth (Fig. 4A). Mean PSA levels in the 1G8-treated mice were 7-, 5-, and 3-fold lower at days 22, 30, and 37, respectively, than in the PBS-control group. At day 51, the mean PSA level in the 1G8-treated mice was 350 ng/ml, which was equivalent approximately to levels in PBS-treated mice at day 30, indicating retardation in tumor growth of approximately 20 days.

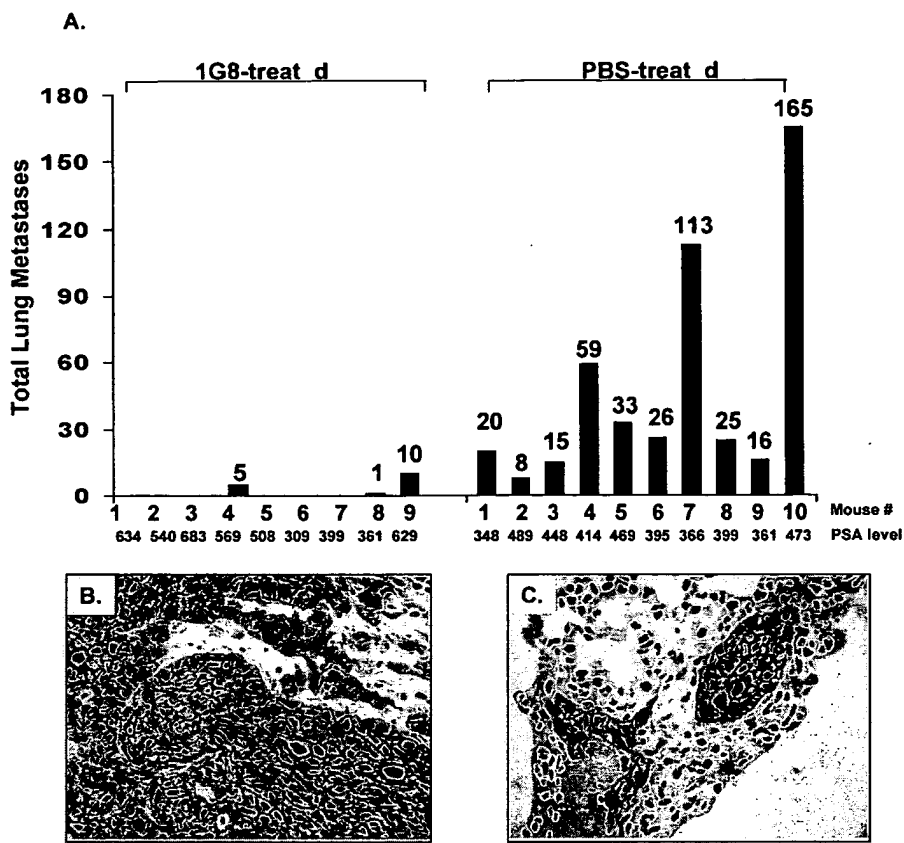


Fig. 5. Anti-PSCA mAb inhibit lung metastasis in mice bearing large orthotopic prostate tumors. Mice with established orthotopic LAPC-9 tumors were treated i.p. with either PBS (control) or 1G8 mAb (1 mg) nine times for 3 weeks. Mice were killed at different times when large prostate tumors were established (PSA >300 ng/ml, see indicated values for each individual mouse). Prostate and lungs were harvested from PBS-treated ($n = 10$) and 1G8-treated ($n = 9$) and processed for IHC analysis by using anti-STEAP antibodies. Total number of lung metastases in five lung sections for each mouse analyzed is shown (A). No metastases were detected in 1G8-treated mice 1, 2, 3, 5, 6, and 7. The photomicrographs demonstrate representative staining of local orthotopic tumors (B) and lung micrometastases (C).

The effect of 1G8 mAb on tumor growth led to a significant prolongation ($P = 0.004$) of survival of the mice. In the 1G8-treated group, the median survival was 89 days (range 77–101 days) vs. 56.5 days (range 42–71 days) in the PBS-treated mice (Fig. 4B), representing a median survival increase of 32.5 days.

We then studied the effect of the 1G8 mAb on mice with a higher tumor burden (PSA levels 64–78 ng/ml). Treatment was comprised of 10 injections of 1 mg 1G8 mAb or PBS over a 4-week period. Survival again was prolonged significantly ($P = 0.002$) in the 1G8-treated group, with a median survival of 78.5 days (range 52–105 days) vs. 40 days (range 32–48 days) in the PBS-treated group (Fig. 4C), representing a median survival increase of 38.5 days. Significant prolongation of survival was detected also by treatment of established orthotopic LAPC-9 tumors with 3C5 mAb ($P = 0.0005$), leading to an increase in median survival by approximately 15 days compared with control mice (Fig. 4D). In all experiments, antibody treatment also showed a prominent effect on the health of the mice. At 5–6 weeks after tumor-cell injection, mice in the control group appeared sickly and cachectic, characterized by sluggishness, an unkempt appearance, and scruffy fur especially around the eyes (data not shown), followed by mortality starting at 5 weeks (Fig. 4). At the same time point, antibody-treated mice appeared healthy and active and maintained normal grooming behavior (data not shown). The health of antibody-treated mice deteriorated at a significantly later time than the control mice, which correlated with their prolonged survival (data not shown).

Anti-PSCA mAbs Prevent Formation of Lung Metastasis from LAPC-9 Orthotopic Tumors. A major advantage of the orthotopic prostate-cancer model is the ability to study the development of metastases. Formation of metastasis in mice bearing established orthotopic tumors was studied by IHC analysis on lung sections using an antibody against a prostate-specific cell-surface protein STEAP expressed at high levels in LAPC-9 xenografts (14). Mice bearing established orthotopic LAPC-9 tumors were administered 11 injections of either 1 mg 1G8 mAb or PBS over a 4-week period. Mice in both groups were allowed to establish a high tumor burden (PSA levels greater than 300 ng/ml), to ensure a high frequency of metastasis formation in mouse lungs. Mice then were killed and their prostate and lungs were analyzed for the presence of LAPC-9 cells by anti-STEAP IHC analysis. Large local prostate tumors expressing STEAP were detected in mice from both groups (Fig. 5B). Metastases were detected readily in all lungs analyzed (8–165 per lung) from the 10 PBS-treated mice analyzed (Fig. 5A and C). In contrast, no micrometastases were detected in the lungs of six of the nine 1G8-treated mice, and only a few micrometastases were scored in the lungs of the other three mice (Fig. 5A). These results demonstrate that anti-PSCA mAb significantly inhibits ($P < 0.0001$) metastasis formation in mice bearing large orthotopic tumor burden (PSA levels 300–650 ng/ml). These striking findings raise the possibility that immunotherapy targeted to PSCA may prevent metastasis formation effectively in patients with established tumors before or after prostatectomy.

Our studies demonstrate a broad anti-tumor efficacy of anti-

PSCA antibodies on initiation and progression of prostate cancer in xenograft mouse models. Anti-PSCA antibodies inhibited tumor formation of both androgen-dependent and androgen-independent tumors as well as retarded the growth of already established tumors significantly and prolonged the survival of treated mice. Moreover, anti-PSCA mAbs demonstrated a dramatic inhibitory effect on the spread of local prostate tumor to distal sites, even in the presence of a large tumor burden. Thus, use of the orthotopic mouse models allowed us to demonstrate significant efficacy of anti-PSCA mAbs on major clinically relevant end points/PSA levels (tumor growth), prolongation of survival, and health.

Anti-prostate tumor activity was demonstrated previously for antibodies directed against the Her-2/Neu (18) and the epidermal growth-factor receptor (EGFR; ref. 19) antigens. Unlike the results obtained with anti-PSCA antibodies, the anti-HER-2/Neu mAb Herceptin affected the growth of androgen-dependent but not androgen-independent xenografts, indicating the necessity for signaling through the androgen receptor for effective Herceptin response (18). The anti-EGFR mAb, C225, significantly inhibited the growth of s.c.-established tumors derived from androgen-independent DU145 and PC3 cells (19).

The mechanism by which the anti-PSCA mAbs exert their effect on the growth of prostate-cancer cells is unknown. Multiple mechanisms have been proposed for the ability of anti-tumor antibodies to mediate their effect *in vivo*, including programmed cell death, differentiation of tumor cells, or modulation of angiogenesis factors (20–23). An alternative mechanism involves disruption of PSCA-mediated cell-cell or cell-matrix interaction that is critical for local tumor growth and spread to distal sites. Such a mechanism has been implicated for another glycosylphosphatidylinositol-linked Ly6-family member tumor antigen E48, which was found to mediate cell-cell interaction in squamous cell carcinomas (24). In addition, the involvement of the effector arm of the immune system in antibody-mediated anti-tumor activity, primarily by engagement with

activation and inhibitory Fc receptors, has been demonstrated (25). The extent to which cell-mediated or complement-dependent effector function mechanisms contribute to the anti-tumor activity exhibited by anti-PSCA mAbs needs to be examined. Similar anti-tumor activity was demonstrated by both 1G8 and 3C5 mAbs, the isotypes of which ($\gamma 1$ and $\gamma 2a$, respectively) differ in their ability to engage the immune system (26, 27). The 1G8 mAb was consistently more efficacious in growth retardation of established orthotopic LAPC-9 tumors, leading to greater prolongation of survival as compared with the 3C5 mAb. These results suggest an intrinsic antibody activity on tumor cells after binding to PSCA, which results in a significantly reduced and long-lasting tumor-growth rate. The increased efficacy exhibited by 1G8 as compared with 3C5 can be attributed to its higher affinity to PSCA and/or to its binding to a unique epitope on the middle domain of PSCA extracellular domain.

PSCA is one of the few largely prostate-specific cell-surface antigens that represent potential antibody therapy targets for prostate cancer. Other antigens include STEAP, an antigen highly expressed in all stages of prostate cancer including advanced hormone-refractory disease (14) and prostate-specific membrane antigen, which is expressed in early and late-stage prostate cancer (28). Of importance is the significant PSCA expression on the majority (80–100%) of patient specimens derived from all stages of the disease including androgen-refractory and metastatic tissues (9). These observations, together with the results presented in this study, validate PSCA as an attractive target for immunotherapy in prostate cancer and demonstrate the potential therapeutic utility of anti-PSCA mAbs for the treatment of recurrent and metastatic disease.

We thank Chris O'Brien and James Kuo for antibody production and characterization, David Myszka for antibody affinity measurements, Dr. Charles Sawyers for comments on the manuscript, and Celeste Jones for assistance in manuscript preparation. This work was supported by UroGenesys, Inc. O.N.W. is an Investigator of the Howard Hughes Medical Institute. R.E.R. and O.N.W. are consultants to UroGenesys, Inc.

1. Lalan, E. N., Laniado, M. E. & Abel, P. D. (1997) *Cancer Metastasis Rev.* **16**, 29–66.
2. Slovin, S. F., Kelly, W. K. & Scher, H. I. (1998) *Semin. Urol. Oncol.* **16**, 53–59.
3. Gregorakis, A. K., Holmes, E. H. & Murphy, G. P. (1998) *Semin. Urol. Oncol.* **16**, 2–12.
4. Holliger, P. & Hoogenboom, H. (1998) *Nat. Biotechnol.* **16**, 1015–1016.
5. Shak, S. (1999) *Semin. Oncol.* **26**, 71–77.
6. McDevitt, M. R., Barendswaard, E., Ma, D., Lai, L., Curcio, M. J., Sgouros, G., Ballangrud, A. M., Yang, W. H., Finn, R. D., Pellegrini, V., et al. (2000) *Cancer Res.* **60**, 6095–6100.
7. Smith-Jones, P. M., Vallabahajosula, S., Goldsmith, S. J., Navarro, V., Hunter, C. J., Bastidas, D. & Bander, N. H. (2000) *Cancer Res.* **60**, 5237–5243.
8. Reiter, R. E., Gu, Z., Watabe, T., Thomas, G., Szigeti, K., Davis, E., Wahl, M., Nisitani, S., Yamashiro, J., Le Beau, M. M., Loda, M. & Witte, O. N. (1998) *Proc. Natl. Acad. Sci. USA* **95**, 1735–1740.
9. Gu, Z., Thomas, G., Yamashiro, J., Shintaku, I. P., Dorey, F., Raitano, A., Witte, O. N., Said, J. W., Loda, M. & Reiter, R. E. (2000) *Oncogene* **19**, 1288–1296.
10. Reiter, R. E., Sato, I., Thomas, G., Qian, J., Gu, Z., Watabe, T., Loda, M. & Jenkins, R. B. (2000) *Genes Chromosomes Cancer* **27**, 95–103.
11. Dannull, J., Diener, P. A., Prikler, L., Furstenberger, G., Cerny, T., Schmid, U., Ackermann, D. K. & Grottrup, M. (2000) *Cancer Res.* **60**, 5522–5528.
12. Craft, N., Chhor, C., Tran, C., Belldegrun, A., DeKernion, J., Witte, O. N., Said, J., Reiter, R. E. & Sawyers, C. L. (1999) *Cancer Res.* **59**, 5030–5036.
13. Kaighn, M. E., Narayan, K. S., Ohnuki, Y., Lechner, J. F. & Jones, L. W. (1979) *Invest. Urol.* **17**, 16–23.
14. Hubert, R. S., Vivanco, I., Chen, E., Rastegar, S., Leong, K., Mitchell, S. C., Madraswala, R., Zhou, Y., Kuo, J., Raitano, A. B., et al. (1999) *Proc. Natl. Acad. Sci. USA* **96**, 14523–14528.
15. Morton, T. A. & Myszka, D. G. (1998) *Methods Enzymol.* **295**, 268–294.
16. Fu, X., Herrera, H. & Hoffman, R. M. (1992) *Int. J. Cancer* **52**, 987–990.
17. Kubota, T. (1994) *J. Cell. Biochem.* **56**, 4–8.
18. Agus, D. B., Scher, H. I., Higgins, B., Fox, W. D., Heller, G., Fazzari, M., Cordon-Cardo, C. & Golde, D. W. (1999) *Cancer Res.* **59**, 4761–4764.
19. Prewett, M., Rockwell, P., Rockwell, R. F., Giorgio, N. A., Mendelsohn, J., Scher, H. I. & Goldstein, N. I. (1996) *J. Immunother. Emphasis Tumor Immunol.* **19**, 419–427.
20. Wu, X., Fan, Z., Masui, H., Rosen, N. & Mendelsohn, J. (1995) *J. Clin. Invest.* **95**, 1897–1905.
21. Sturgis, E. M., Sacks, P. G., Masui, H., Mendelsohn, J. & Schantz, S. P. (1994) *Otolaryngol. Head Neck Surg.* **111**, 633–643.
22. Modjtahedi, H., Eccles, S., Sandie, J., Box, G., Titley, J. & Dean, C. (1994) *Cancer Res.* **54**, 1695–1701.
23. Petit, A. M., Rak, J., Hung, M. C., Rockwell, P., Goldstein, N., Fendly, B. & Kerbel, R. S. (1997) *Am. J. Pathol.* **151**, 1523–1530.
24. Schrijvers, A. H., Gerretsen, M., Fritz, J. M., van Walsum, M., Quak, J. J., Snow, G. B. & van Dongen, G. A. (1991) *Exp. Cell Res.* **196**, 264–269.
25. Clynes, R. A., Towers, T. L., Presta, L. G. & Ravetch, J. V. (2000) *Nat. Med.* **6**, 443–446.
26. Masui, H., Moroyama, T. & Mendelsohn, J. (1986) *Cancer Res.* **46**, 5592–5598.
27. Fan, Z. & Mendelsohn, J. (1998) *Curr. Opin. Oncol.* **10**, 67–73.
28. Israeli, R. S., Powell, C. T., Fair, W. R. & Heston, W. D. (1993) *Cancer Res.* **53**, 227–230.

Prostate Stem Cell Antigen Is Overexpressed in Human Transitional Cell Carcinoma¹

Nordine Amara,² Ganesh S. Palapattu,² Matthew Schrage, Zhennan Gu, George V. Thomas, Fred Dorey, Jonathan Said, and Robert E. Reiter³

Departments of Urology [N. A., G. S. P., Z. G., R. E. R.], Pathology [M. S., G. V. T., J. S.], and Orthopedics [F. D.], and Jonsson Cancer Center [N. A., G. S. P., Z. G., R. E. R.], University of California-Los Angeles School of Medicine, Los Angeles, California 90095

Abstract

Prostate stem cell antigen (PSCA), a homologue of the Ly-6/Thy-1 family of cell surface antigens, is expressed by a majority of human prostate cancers and is a promising target for prostate cancer immunotherapy. In addition to its expression in normal and malignant prostate, we recently reported that PSCA is expressed at low levels in the transitional epithelium of normal bladder. In the present study, we compared the expression of PSCA in normal and malignant urothelial tissues to assess its potential as an immunotherapeutic target in transitional cell carcinoma (TCC). Immunohistochemical analysis of PSCA protein expression was performed on tissue sections from 32 normal bladder specimens, as well as 11 cases of low-grade transitional cell dysplasia, 21 cases of carcinoma *in situ* (CIS), 38 superficial transitional cell tumors (STCC, stages T₁-T₂), 65 muscle-invasive TCCs (ITCCs, stages T₂-T₄), and 7 bladder cancer metastases. The level of PSCA protein expression was scored semiquantitatively by assessing both the intensity and frequency (*i.e.*, percentage of positive tumor cells) of staining. We also examined PSCA mRNA expression in a representative sample of normal and malignant human transitional cell tissues. In normal bladder, PSCA immunostaining was weak and confined almost exclusively to the superficial umbrella cell layer. Staining in CIS and STCC was more intense and uniform than that seen in normal bladder epithelium ($P < 0.001$), with staining detected in 21 (100%) of 21 cases of CIS and 37 (97%) of 38 superficial tumors. PSCA protein was also detected in 42 (65%) of 65 of muscle-invasive and 4 (57%) of 7 metastatic cancers, with the highest levels of PSCA expression (*i.e.*, moderate-strong staining in >50% of tumor cells) seen in 32% of invasive and 43% of metastatic samples. Higher levels of PSCA expression correlated with increasing tumor grade for both STCCs and ITCCs ($P < 0.001$). Northern blot analysis confirmed the immunohistochemical data, showing a dramatic increase in PSCA mRNA expression in two of five muscle-invasive transitional cell tumors when compared with normal samples. Confocal microscopy demonstrated that PSCA expression in TCC is confined to the cell surface. These data demonstrate that PSCA is overexpressed in a majority of human TCCs, particularly CIS and superficial tumors, and may be a useful target for bladder cancer diagnosis and therapy.

Introduction

TCC⁴ of the bladder poses a significant worldwide clinical problem, with an estimated 54,200 new cases and 12,100 associated deaths reported in the United States in 1999 alone (1). The majority of

patients present initially with superficial disease limited to the urothelium or lamina propria of the bladder wall. Such lesions are often amenable to transurethral resection. Intravesical immunotherapy with BCG may prevent recurrence or progression of high-risk tumors (*e.g.*, high grade or T₁) and CIS (2). However, despite these efforts, ~50% of superficial tumors will continue to recur and as many as 30% will progress to muscle-invasive disease (3). Although radical cystectomy can salvage many patients with muscle-invasive cancers, a significant number go on to die from metastatic disease, for which there is currently no effective treatment. These data underscore the urgent necessity for better diagnostic and treatment strategies for superficial and invasive bladder cancers.

Given the sensitivity of bladder cancer to BCG immunotherapy, there is a particular need to identify bladder cancer antigens for cellular and monoclonal antibody-based targeted immunotherapies. EGFR, for example, is overexpressed by a significant percentage of muscle-invasive bladder cancers (4). A recent study demonstrated that monoclonal antibody directed against EGFR slowed growth of a human transitional cell cancer in an orthotopic mouse model (5). Similarly, new bladder cancer markers have been identified that not only demonstrate high specificity for TCC but that also show early promise as a clinical tool. One such marker, uroplakin II, is an urothelium-specific differentiation antigen that is expressed by ~40% of TCCs (6). Detection of uroplakin-positive cells in human sera has been associated with metastatic spread of bladder cancer cells and may identify patients with micrometastatic spread prior to undergoing cystectomy (7).

PSCA is a glycosylphosphatidylinositol (GPI)-anchored 123-amino-acid glycoprotein related to the Ly-6/Thy-1 family of cell surface antigens (8). PSCA expression in normal tissues is largely prostate-specific, but we recently reported finding PSCA transcripts and protein in transitional epithelium of the bladder and neuroendocrine cells of the stomach (9). *In situ* hybridization and IHC analyses demonstrated PSCA expression in more than 80% of local and 100% of bone-metastatic prostate cancer specimens (9). Importantly, the intensity of PSCA expression increased with tumor grade and stage, which suggests its potential as an immunotherapeutic target for high-risk and metastatic prostate cancer. Supporting this hypothesis, we recently demonstrated that monoclonal antibodies against PSCA can inhibit tumor growth and metastasis formation and can prolong survival in mice bearing human prostate cancer xenografts (10). Also, Dannull *et al.* (11) recently reported that a PSCA-derived peptide could elicit a PSCA-specific T-cell response in a patient with metastatic prostate cancer.

Because PSCA is present at low levels in normal bladder, we asked whether PSCA is expressed in TCC. We also determined whether PSCA is overexpressed in bladder cancer compared with normal bladder and whether the level of expression correlates with bladder cancer stage or grade. We demonstrate that PSCA is expressed by a majority of both muscle-invasive and superficial tumors. Moreover,

Received 2/2/01; accepted 4/27/01.

The costs of publication of this article were defrayed in part by the payment of page charges. This article must therefore be hereby marked *advertisement* in accordance with 18 U.S.C. Section 1734 solely to indicate this fact.

¹ Supported in part by grants from the NIH K08 CA74169, the Cancer Research Institute, and CaPCURE.

² N. A. and G. S. P. contributed equally to this work.

³ To whom requests for reprints should be addressed, at the Department of Urology, UCLA, 66-134 Center for the Health Sciences, 10833 Le Conte Avenue, Los Angeles, CA 90095-1738. E-mail: reiter@mednet.ucla.edu.

⁴ The abbreviations used are: TCC, transitional cell carcinoma; PSCA, prostate stem cell antigen; ITCC, invasive TCC; STCC, superficial TCC; CIS, carcinoma *in situ*; IHC, immunohistochemical; BCG, Calmette-Guerin bacillus; EGFR, epidermal growth factor receptor.

PSCA is overexpressed in virtually all nonmuscle invasive bladder tumors and in >30% of invasive and metastatic cancers. As with prostate cancer, expression increases with increasing tumor grade. Interestingly, the overexpression of PSCA that we observed in TCC is quantitatively more than that seen in prostate cancer with respect to tumor stage. These results support PSCA as a potential diagnostic and/or therapeutic target in bladder cancer.

Materials and Methods

Tissue Samples

All of the tissue specimens were obtained with permission from the Human Tissue Resources Committee of the Department of Pathology at University of California-Los Angeles Medical Center. One hundred seventy-four formalin-fixed, paraffin-embedded human bladder tissues were obtained from 135 different patients. Blocks were then cut into 4- μ m sections and mounted on charged slides in the usual fashion. H&E-stained sections of the neoplasms were graded by an experienced urological pathologist according to the criteria set forth in the International Histological Classification of Tumors. Staging was performed based on the 1997 Tumor-Node-Metastasis classification system. The tissue samples consisted of 32 normal bladder samples, 11 cases of low-grade transitional cell dysplasia, 21 cases of CIS, 38 cases of STCC (stages T₀-T₁), 65 cases of muscle-ITCC, (stages T₂-T₄), and 7 metastases (6 lymph nodes, 1 lung). Normal bladder samples were obtained from cystectomy specimens of patients with focal muscle-invasive disease and no preoperative cystoscopic or cytological evidence of CIS. Areas histologically free of tumor were taken as normal bladder tissue. Of the specimens in the STCC group, 13 were grade II and 25 were grade III. One sample in the ITCC group was grade I, 12 were grade II, and 53 were grade III.

Immunohistochemistry

Methodology. Specimens were stained using modifications of an immunoperoxidase technique previously described (12). Briefly, antigen retrieval was performed on paraffin sections using a commercial steamer and 0.01 M citrate buffer (pH 6.0). Slides were then washed in PBS and incubated with normal horse serum, diluted 1:20, for 10 min. PSCA monoclonal antibody 1G8 was generated in the CellPharm System 100 as described previously (9). Monoclonal antibodies to PSCA were diluted 1:20 in PBS. After 50 min of incubation with the primary antibody, slides were treated sequentially with rabbit antimouse immunoglobulin, swine antirabbit immunoglobulin, and rabbit antiswine immunoglobulin (all biotin conjugated). Slides were then incubated with streptavidin-peroxidase, and antibody localization was performed using the diaminobenzidine reaction. Positive and negative controls were performed on tissues obtained from mouse xenograft tumors that were derived from the human prostate cancer cell lines LAPC-9 and PC3, respectively. Negative controls for each stained section consisted of substitution of the primary antibody by a non-cross-reacting isotype-matched monoclonal antibody.

Scoring Methods. Histopathological slides of the clinical specimens were read and scored by two pathologists (G. V. T., and J. S.) in a blinded fashion. There was a >90% inter- and intraobserver agreement. IHC intensity was graded on a scale of 0 to 3+ (0, no staining; 1+, mildly intense; 2+, moderately intense; 3+, severely intense). Staining density was quantified as the percentage of cells staining positive with the primary antibody, as follows: 0 = no staining, 1 = superficial staining, 2 = positive staining in <25% of the sample; 3 = positive staining in 25-50% of the sample; 4 = positive staining in >50% of the specimen; and 5 = positive staining throughout the sample. Intensity score (0 to 3+) was multiplied by the density score (0-5) to calculate an overall score (0-15). In this way, we were able to differentiate specimens that may have had focal areas of increased staining from those that had diffuse areas of increased staining (13). The overall score for each specimen was then categorically assigned to one of the following groups: 0-3 (little to no immunoreactivity), 4-7 (moderate immunoreactivity), and 8-15 (strong immunoreactivity). The above groupings attempt to stratify the overall PSCA immunoreactivity of each specimen for the purpose of comparison. Overexpression was considered to be present when the overall score was ≥ 8 , indicating that 50-100% of cells had moderate or intense staining. Within any

given slide, adjacent areas of normal transitional epithelium were used as positive internal controls.

Northern Blot Analysis. Fresh human tissues were obtained at the time of surgery, and RNA was prepared according to the manufacturer's recommendations (Biotecx, Houston, TX). Nine samples were obtained: four benign and five malignant transitional cell tissues. All five malignant tissues were from patients with muscle-invasive disease. Normal bladder RNA was obtained from benign areas of cystectomy specimens of patients with focal muscle-ITCC. In none of these patients was there evidence, either pre- or postoperatively, of CIS. Northern blot analysis was then performed as described previously (14). Briefly, 10 μ m of RNA from each sample were loaded onto a 1% agarose gel. Equal loading and RNA integrity was confirmed by ethidium bromide staining. After electrophoresis, RNA samples were transferred onto a nitrocellulose membrane. The PSCA probe was prepared from a cDNA fragment using random oligonucleotide primers (Amersham) and was labeled with [³²P]dCTP. Equal loading of RNA was also confirmed by hybridization with an actin probe. The human prostate cancer cell lines LAPC-4 and LNCaP were used as positive and negative controls, respectively. Preparation of total RNA from cell lines was performed according to the manufacturer's instructions (Biotecx). The human bladder cancer cell line HT1376 was also included in the analysis.

Confocal Microscopy. Human bladder cancer cell line HT1376 cells were washed with PBS containing 1 mM MgCl₂ and 0.1 mM CaCl₂ (PBS/CM). Cells were incubated with the primary antibody, murine monoclonal anti-PSCA antibody 1G8, and subsequently with a secondary antibody, fluorescein-conjugated FITC goat antimouse IgG (1:200; Jackson ImmunoResearch, West Grove, PA). The cells were then fixed with 2% paraformaldehyde in PBS/CM for 30 min. Next, the cells were incubated with 50 mM NH₄Cl in PBS/CM for 10 min at room temperature and permeabilized for 10 min with 0.075% (w/v) saponin in PBS/CM containing 0.2% BSA. Nuclei were counterstained with propidium iodide (1 μ g/ml; Sigma Chemical Co.). Optical sections were obtained by laser confocal microscopy.

Statistical Analysis. Overall scores of PSCA staining were evaluated with respect to tissue histology using a one-way ANOVA-Sidak multiple comparison procedure, using overall score as the dependent variable and the histopathological subgroup as the factor. Table 3 was constructed in this manner. To evaluate the relationship between tumor grade and overall score within the subgroups STCC and ITCC, we performed a two-way ANOVA using the overall score as the dependent variable and the grade and subgroup as the two factors. The results of this analysis can be seen in Table 2. For all analyses, $P < 0.05$ was considered statistically significant.

Results

PSCA Protein Expression in Normal, Dysplastic, and Malignant Urothelium. The expression pattern of PSCA in normal bladder tissues and TCCs of different stages and grades is summarized in Tables 1 and 2 and illustrated in Fig. 1, A-H. Thirty of 32 normal bladder specimens stained positively for PSCA. In these samples, PSCA expression was generally weak (*i.e.*, 1+) and was localized almost exclusively to the superficial umbrella cell layer (*i.e.*, density score of 1; Fig. 1A). The mean intensity, density, and overall staining scores from normal tissues were 1.0, 1.0, and 1.1, respectively (Table 1). Expression of PSCA in normal bladders was significantly less than that found in CIS and both invasive and superficial tumors ($P = 0.001$; Table 3).

PSCA expression was detected in all of the 11 low-grade dysplasia specimens surveyed (Table 1; IHC data not shown). The mean intensity, density, and overall score for these samples was 1.8, 2.0, and 3.6, respectively. Although PSCA staining intensity and density tended to be higher in dysplastic than in normal bladder, this was not statistically significant ($P = 0.782$; Table 3). In contrast, PSCA expression in CIS was intense and homogeneous in all but two specimens (19 of 21), with a mean intensity, density, and overall score of 2.7, 4.9, and 13.2, respectively (Table 1). Whereas PSCA staining in normal and dysplastic bladders was confined to the most superficial layers of urothelium, staining in CIS was detected in all of the neoplastic

Table 1 Comparison of IHC staining intensity, density, and overall score by stage

	Intensity					Density					Overall Score					
	0	1+	2+	3+	Mean \pm SD	0	1	2	3	4	5	Mean \pm SD	0-3	4-7	8-15	Mean \pm SD
Normal, n = 32 (100%)	2 (6)	28 (88)	2 (6)	0 (0)	1.0 \pm 0.4	2 (6)	28 (88)	2 (6)	0 (0)	0 (0)	0 (0)	1.0 \pm 0.4	32 (100)	0 (0)	0 (0)	1.1 \pm 0.8
Dysplasia, n = 11 (100%)	0 (0)	5 (45)	3 (27)	3 (27)	1.8 \pm 0.9	0 (0)	0 (0)	11 (100)	0 (0)	0 (0)	0 (0)	2.0 \pm 0.0	5 (45)	6 (55)	0 (0)	3.6 \pm 1.7
CIS, n = 21 (100%)	0 (0)	2 (10)	3 (14)	16 (76)	2.7 \pm 0.7	0 (0)	0 (0)	1 (5)	0 (0)	0 (0)	20 (95)	4.9 \pm 0.7	1 (5)	1 (5)	19 (90)	13.2 \pm 3.7
Superficial TCC																
T _a , n = 19 (100%)	0 (0)	4 (21)	11 (58)	4 (21)	2.0 \pm 0.7	0 (0)	0 (0)	3 (16)	2 (11)	5 (26)	9 (47)	4.1 \pm 1.1	4 (21)	1 (5)	14 (74)	8.6 \pm 4.2
T ₁ , n = 19 (100%)	1 (5)	2 (11)	8 (42)	8 (42)	2.2 \pm 0.9	1 (5)	0 (0)	0 (0)	1 (5)	1 (5)	16 (84)	4.6 \pm 1.2	1 (5)	3 (16)	15 (79)	10.7 \pm 4.5
Invasive TCC																
T ₂ , n = 19 (100%)	6 (32)	4 (21)	5 (26)	4 (21)	1.4 \pm 1.2	6 (32)	0 (0)	6 (32)	4 (21)	2 (11)	1 (5)	1.9 \pm 1.6	9 (47)	6 (32)	4 (21)	4.1 \pm 4.1
T ₃ , n = 39 (100%)	15 (39)	6 (15)	6 (15)	12 (31)	1.4 \pm 1.3	15 (39)	0 (0)	3 (8)	6 (15)	6 (15)	9 (23)	2.4 \pm 2.1	17 (44)	9 (23)	13 (33)	5.5 \pm 5.6
T ₄ , n = 7 (100%)	2 (29)	0 (0)	1 (14)	4 (57)	2.0 \pm 1.4	2 (29)	0 (0)	1 (14)	3 (43)	0 (0)	1 (14)	2.3 \pm 1.8	2 (29)	1 (14)	4 (57)	6.6 \pm 5.5
Metastasis, n = 7 (100%)	3 (43)	1 (14)	0 (0)	3 (43)	1.4 \pm 1.5	3 (43)	0 (0)	1 (14)	0 (0)	1 (14)	2 (29)	2.3 \pm 2.4	4 (57)	0 (0)	3 (43)	6.3 \pm 7.3

urothelial cell layers (Fig. 1B). Overall, CIS expressed significantly higher levels of PSCA than any other specimen category in this study ($P < 0.05$, compared with normal bladder, dysplasia, STCC, ITCC, and metastases; Table 3).

Nomuscle invasive tumors (stages T_a and T₁) also displayed an overall strong positivity for PSCA expression (Fig. 1C). Twenty-nine (76%) of 38 samples overexpressed PSCA, defined as an overall score of ≥ 8 (Table 1). The mean intensity, density, and overall scores for T_a tumors were 2.0, 4.1, and 8.6, respectively, whereas T₁ lesions scored 2.2, 4.6, and 10.7, respectively. As a group, superficial tumors stained more strongly than normal, dysplastic, and invasive samples ($P = 0.001$; Table 3). PSCA expression increased significantly with worsening tumor grade in nonmuscle invasive tumors (Table 2). Grade 2 lesions had a mean overall staining score of 6.8 compared with a mean score of 11.2 for Grade 3 tumors ($P < 0.001$).

We detected PSCA expression in 42 (65%) of 65 muscle-invasive tumors, of which 21 (32%) exhibited the highest levels of expression (*i.e.*, overall score, ≥ 8). Locally advanced tumors tended to express higher levels of PSCA than organ-confined lesions, although this trend did not reach statistical significance. T₂ tumors had a mean overall score of 4.1, whereas T₃ and T₄ tumors had mean intensity *versus* density scores of 5.5 and 6.6, respectively (Table 1; Fig. 1, D-F). As with superficial tumors, PSCA expression in muscle-invasive cancers increased significantly with tumor grade (Table 2). Eight (67%) of 12 grade 2 tumors displayed no detectable PSCA expression, whereas only 14 (27%) of 53 grade 3 lesions showed no expression. The mean overall score for grade 2 muscle-invasive tumors was 2.1, compared with a score of 5.9 for grade 3 tumors ($P < 0.001$). Several poorly differentiated muscle-invasive TCCs contained foci of squamous cell differentiation. PSCA expression in these cases was particularly prominent, as depicted in Fig. 1F. We also examined seven bladder cancer metastases. Four (57%) stained positive for PSCA (Fig. 1G), three of which were in the strongest immunoreactivity category (Table 1). The mean intensity, density, and overall scores for metastases were 1.4, 2.3, and 6.3, respectively. These results demonstrate that PSCA is expressed by a majority of TCCs. Expression is greatest in CIS and superficial tumors but is also extremely high in

>30% of muscle-invasive and metastatic lesions. Importantly, within the subgroups STCC and ITCC, higher levels of PSCA expression correlate significantly with increasing tumor grade.

PSCA Protein Is Expressed on the Cell Surface of Bladder Cancer Cells. To confirm that PSCA localizes to the cell surface of bladder cancer cells, we stained nonpermeabilized HT1376 bladder cancer cells and examined them by confocal microscopy. PSCA monoclonal antibody 1G8 detected PSCA expression in a subpopulation of these cells. As seen in Fig. 1H, PSCA protein expression is localized to the cell surface.

PSCA mRNA Expression in Normal and Malignant Urothelium. Northern blot analysis was performed on four normal and five invasive transitional cell cancer samples (Fig. 1I). As predicted, low levels of PSCA mRNA expression were detected in three of four normal bladder specimens. PSCA mRNA was also detected in three (60%) of five muscle-invasive tumors and an invasive transitional cell cancer cell line (HT1376). Consistent with the IHC findings, two of these invasive cancers (*i.e.*, 40%) overexpressed PSCA when compared with normal bladder. The level of PSCA expression in these two cases was similar to that seen in LAPC 9, a prostate cancer xenograft. The corresponding IHC stain for a patient with a muscle-invasive transitional cell tumor of the renal pelvis is shown in Fig. 1E (lane with asterisk) and confirms the intense expression detected by Northern analysis. Of all of the tissues examined in this study, this was the only sample to be obtained from a site other than the bladder.

Discussion

PSCA is a cell surface antigen that has potential utility in the diagnosis and treatment of prostate cancer. In the present study, we demonstrate that PSCA is also expressed in normal bladder and in a large percentage of human TCCs. Interestingly, we found that expression in normal bladder is limited to the umbrella cell layer, a differentiated cell type believed to play a role in maintaining the integrity of the urothelium. Although the function of PSCA remains unknown, homologues of PSCA have been implicated in homotypic cell adhesion (15). Bahrenberg *et al.* (16) recently reported that PSCA expres-

Table 2 Comparison of IHC staining intensity, density, and overall score by grade

	Intensity					Density					Overall score					
	0	1+	2+	3+	Mean \pm SD	0	1	2	3	4	5	Mean \pm SD	0-3	4-7	8-15	Mean \pm SD
STCC (stages T _a -T ₁)																
Grade 2, n = 13 (100%)	1 (7.7)	4 (31)	8 (62)	0	1.5 \pm 0.6	1 (8)	0	2 (15)	0	3 (23)	7 (54)	3.9 \pm 1.6	3 (23)	2 (15)	8 (62)	6.8 \pm 3.5 ^a
Grade 3, n = 25 (100%)	0	2 (8)	11 (44)	12 (48)	2.4 \pm 0.6	0	0	1 (4)	3 (12)	3 (3)	18 (72)	4.5 \pm 0.9	2 (8)	2 (8)	21 (84)	11.2 \pm 4.1 ^a
ITCC (stages T ₂ -T ₄)																
Grade 1, n = 1 (100%)	1 (100)	0	0	0	0.0 \pm 0.0	1 (100)	0	0	0	0	0	0.0 \pm 0.0	1 (100)	0	0	0.0 \pm 0.0
Grade 2, n = 12 (100%)	8 (67)	2 (17)	1 (8)	1 (8)	0.6 \pm 1.0	8 (67)	0	2 (17)	1 (8)	0	1 (8)	1.0 \pm 1.7	10 (83)	1 (8.3)	1 (8.3)	2.1 \pm 4.4 ^a
Grade 3, n = 52 (100%)	14 (27)	8 (15)	11 (21)	19 (37)	1.6 \pm 1.2	14 (27)	0	8 (15)	12 (23)	8 (15)	10 (19)	2.6 \pm 1.8	17 (33)	17 (33)	18 (34)	5.9 \pm 5.1 ^a

^a Two-way ANOVA using staining overall score as the dependent variable and grade and histopathologic subgroup (*i.e.*, non-ITCC and ITCC) as factors was performed. Within each subgroup, higher grade correlated with higher overall score ($P = 0.0002$).

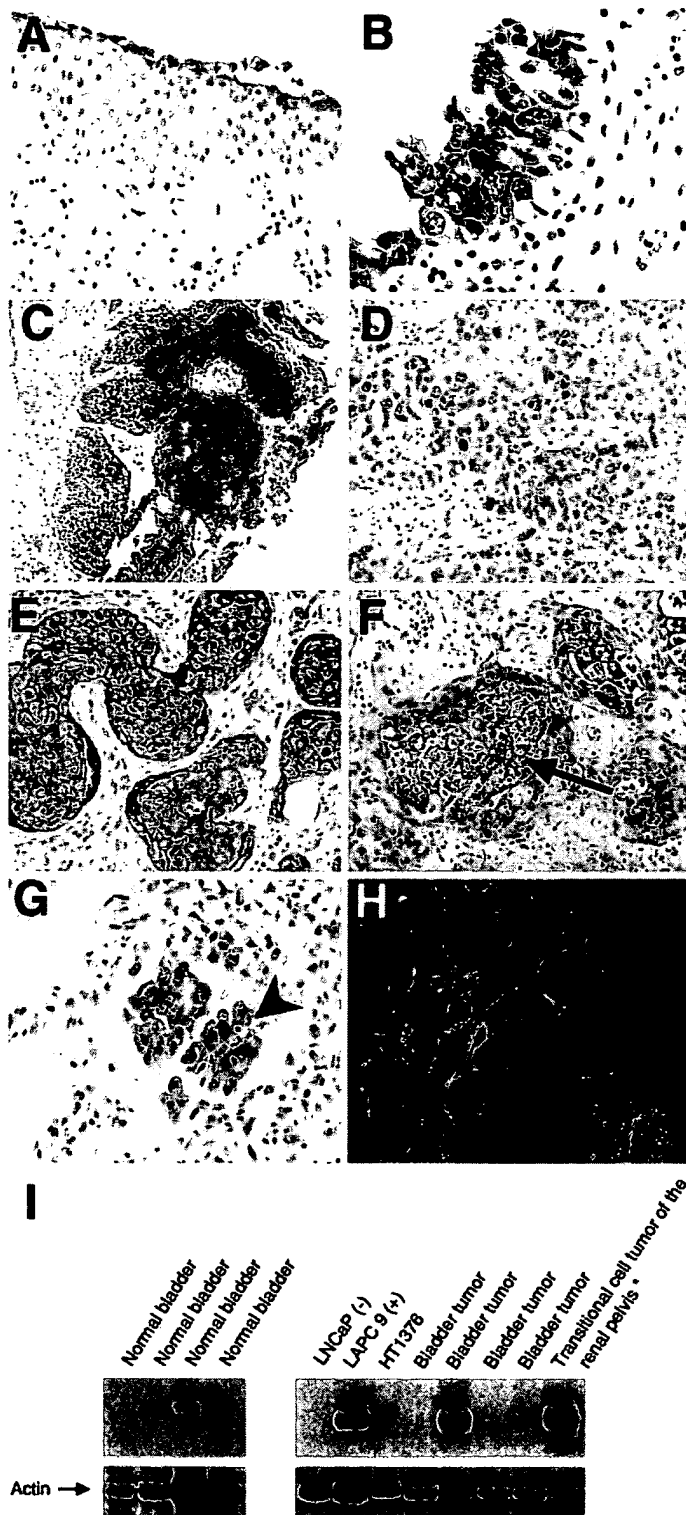


Fig. 1. IHC staining and Northern analysis of PSCA in benign and malignant urothelial tissue. All of the sections were stained with PSCA monoclonal antibody 1G8. *Brown* color, positive stain. *A*, normal bladder tissue displayed weak, superficial staining. *B*, intense, homogeneous staining was seen in CIS specimens. Positive staining can be seen in all layers of neoplastic urothelium. *C*, nonmuscle invasive superficial TCCs showed prominent PSCA expression. *D* and *E*, high-grade muscle-invasive transitional cell tumors displayed moderate-to-strong PSCA immunoreactivity. PSCA mRNA analysis from the tumor in *E* may be seen in *I*, Lane with asterisk. *F*, high-grade muscle-invasive tumors occasionally contained areas of squamous cell differentiation that were hot spots of PSCA expression (arrow). *G*, several metastatic tumors, as seen in this example from a metastatic lesion to the lung, displayed significant PSCA expression. Note the intensely positive island of metastatic transitional cells (arrowhead) surrounded by normal lung parenchyma. *H*, immunofluorescent staining of the cell line HT1376 shows PSCA expression (green, fluorescein) exclusively at the cell surface. Positive staining was seen in only a subpopulation of cells. The nuclei are counterstained with propidium iodide.

Table 3 One-way ANOVA:^a mean overall score versus histopathology

	Absolute difference of the mean overall score <i>P</i>				
	Normal	Low-grade dysplasia	CIS	STCC	ITCC
Dysplasia	2.5 0.782				
CIS	12.1 0.001 ^b	9.6 0.001 ^b			
STCC	8.6 0.001 ^b	6.0 0.001 ^b	3.5 0.046 ^b		
ITCC	4 0.001 ^b	1.5 0.992	8.0 0.001 ^b	4.5 0.001 ^b	
Metastases	5.2 0.066	2.6 0.968	6.9 0.005 ^b	3.4 0.581	1.1 1.000

^a One-way ANOVA-Sidak multiple comparison procedure using mean immunostaining overall score as the dependent variable and grade and histopathological subgroup as factors.

^b Statistically significant.

sion may be regulated by cell-cell contact. It will be important to determine whether PSCA plays a role in normal bladder function and whether PSCA expression is altered in disease states such as interstitial cystitis, which are characterized by a breakdown in the normal urothelial barrier.

PSCA expression was strongest and most common in superficial, nonmuscle invasive tumors. PSCA expression was detected in all but one case of superficial transitional cell cancer and all cases of CIS. Similarly, 90% of CIS specimens and 76% of nonmuscle invasive cancers overexpressed PSCA. In contrast, 35% of invasive cancers had no detectable expression of PSCA, and only 32% overexpressed it. It is unlikely that the failure to detect expression in many invasive cancers was antibody- or antigen-related, because a similar percentage of tumors had no expression on Northern analysis. It is also unlikely that loss of expression can be attributed to a loss of differentiation in muscle-invasive tumors, as was recently proposed by Bahrenberg *et al.*, because the highest levels of PSCA expression were found in CIS, a poorly differentiated and aggressive lesion. Similarly, PSCA expression was higher in poorly differentiated nonmuscle invasive tumors than in differentiated superficial ones. Although it is possible that the loss of PSCA expression is associated with invasion, 32% of invasive and 43% of metastatic tumors overexpressed PSCA. Additional studies will be needed to understand PSCA gene regulation during the process of bladder cancer invasion.

As noted above, increasing levels of PSCA expression correlated with increasing tumor grade in both superficial and muscle-invasive tumors. One possible mechanism for PSCA overexpression is that it may result from PSCA gene amplification. PSCA maps distal to the *MYC* oncogene on chromosome 8q24.2 (8). In prostate cancer, PSCA overexpression is associated with PSCA and *MYC* coamplification (17). Christoph *et al.* (18) and Sauter *et al.* (19) have shown that low-level *MYC* amplification is a common feature of both nonmuscle-invasive and invasive bladder cancers and correlates with worsening tumor grade. Fluorescent *in situ* studies of bladder cancers should clarify whether PSCA overexpression is caused by gene amplification. Also, it will be interesting to determine whether PSCA overexpression correlates with *MYC* amplification.

We observed intense PSCA staining in poorly differentiated transi-

(red). *I*, Northern blot analysis of PSCA expression in normal and malignant urothelium. Three of four normal bladder specimens showed weak PSCA mRNA expression. The human bladder cancer line HT1376 displayed weak PSCA expression. Two of five muscle-invasive TCCs expressed high levels of PSCA mRNA when compared with normal bladder. Weak expression of PSCA was seen in an additional bladder tumor. All of the transitional cell tumors were muscle invasive. The human prostate cancer cell lines LNCaP and LACP 9 were used as negative and positive controls, respectively. See "Results" for discussion of sample that was labeled with asterisk.

sitional cell tumors with squamous features, which suggests that PSCA expression may be associated with squamous differentiation. We recently created a transgenic mouse model using the PSCA promoter to drive green fluorescent protein (GFP) expression.⁵ In this model, we noted GFP expression in keratinized skin as well as in the adult urothelium of a single founder line. Likewise, Bahrenberg *et al.* (16) recently reported that PSCA is expressed by keratinocytes in tissue culture, although we have not seen PSCA expression in adult skin. These observations suggest that PSCA may be a marker of both transitional and squamous differentiation patterns in the bladder and may provide another possible mechanism whereby PSCA expression levels may increase in poorly differentiated bladder tumors.

Our results differ somewhat from those reported recently by Bahrenberg *et al.* (16). Similar to Bahrenberg, we saw dramatically increased levels of PSCA expression in superficial tumors. Likewise, we saw lesser overall expression of PSCA in muscle-invasive tumors. However, unlike Bahrenberg, we found that a majority of invasive and metastatic tumors expressed PSCA and >30% overexpressed it. In addition, although Bahrenberg *et al.* concluded that PSCA expression was a marker of differentiated bladder tumors, we found that PSCA expression was highest in poorly differentiated invasive and superficial tumors. One possible reason for these differences is that the study of Bahrenberg *et al.* did not include cases of CIS or high-grade superficial cancer. Also, their study was small and included only two well-differentiated (presumably superficial) and eight poorly differentiated (presumably invasive) cancers.

Another difference between this study and that of Bahrenberg is that we primarily evaluated PSCA protein expression, whereas the latter looked at mRNA levels exclusively. Importantly, Bahrenberg *et al.* reported finding several PSCA splice variants. One of these, denoted $\Delta(1-17)$, results in the substitution of the 17-amino-acid signal sequence of exon 1 with a new 31-amino-acid sequence. This splice variant is transcribed and would be predicted to contain the epitope in exon 2 that is recognized by PSCA monoclonal antibody 1G8. It is possible, therefore, that, in at least some instances, our immunostaining would have detected a PSCA splice variant. That said, we did not detect any aberrant messages by Northern analysis, and we were clearly able to correlate PSCA mRNA and protein expression in a patient with muscle-invasive TCC. Also, our Northern analysis was consistent with the IHC data, showing expression in 60% of cases and overexpression in 40%.

Confocal microscopy studies demonstrated cell surface expression of PSCA in a subset of cells from the bladder cancer cell line HT1376. IHC analysis of PSCA shows cell surface as well as apparent cytoplasmic staining of PSCA in benign and malignant transitional epithelia (Fig. 1, A-G). One possible explanation for this is that anti-PSCA antibody can recognize PSCA peptide precursors that reside in the cytoplasm. In addition, it is possible that the positive staining that appears in the cytoplasm is actually from the overlying cell membrane. We have observed similar results with prostate cancer *vis-a-vis* confocal/immunofluorescent and IHC data (9). These data seem to indicate that PSCA is a novel cell surface marker for TCC.

Our results suggest that PSCA may have a number of potential uses in the diagnosis and treatment of human TCC. Because neoplastic transitional cells are naturally sloughed from the bladder, differential expression of PSCA in voided samples might form the basis for a diagnostic test. Detection of PSCA on the surface of circulating cells in blood and bone marrow might be useful in identifying some

patients with bladder cancer micrometastases, particularly those whose primary tumors express PSCA. We have recently shown that immunomagnetic beads conjugated with PSCA monoclonal antibodies can detect as few as 1 in 10^7 PSCA-positive cells in bone marrow.⁶ Similar approaches have been tested using uroplakin II as a marker of metastatic transitional cells (7).

PSCA might also be a valuable target for bladder cancer immunotherapy. One potential approach is to use monoclonal antibodies intravesically to treat localized disease (particularly CIS) or systemically to treat advanced disease. We have recently shown that naked PSCA antibodies inhibit prostate cancer tumorigenesis and metastasis, which suggests that they may have utility in TCC as well (10). Similar approaches have been reported in bladder cancer using antibodies against EGFR systemically and against the MUC 1 mucin antigen intravesically (5, 20). PSCA might also be useful for local or systemic vaccine approaches. Dannull *et al.* (11) recently demonstrated that amino acids 14–22 of PSCA can elicit a PSCA-specific T-cell response in a patient with prostate cancer. Given the profound immunosensitivity of bladder cancer to non-specific agents such as BCG, this is a particularly promising approach, especially in the local setting.

In summary, we have shown in this study that PSCA is expressed by a majority of superficial and muscle-invasive transitional cell tumors. Furthermore, PSCA is overexpressed in a majority of superficial tumors and a significant percentage of invasive and metastatic transitional cell cancers. These results suggest that PSCA may be a valuable target for bladder cancer diagnosis and therapy.

References

- Landis, S. H., Murray, T., Bolden, S., and Wingo, P. A. Cancer statistics, 1999. *Cancer J. Clin.*, 9: 8–31, 1999.
- Pow-Sang, J. M., and Seigne, J. D. Contemporary management of superficial bladder cancer. *Cancer Control*, 7: 335–339, 2000.
- Messing, E. M., and Catalona, W. Urothelial tumors of the urinary tract. In: P. W. Walsh, A. B. Retik, E. D. Vaughan, and A. J. Wein (eds.), *Campbell's Urology*, pp. 2327–2391. Philadelphia: W. B. Saunders Company, 1998.
- Koenig, F., Klaus, J., Schorr, D., and Loening, S. A. Urinary markers of malignancy. *Clin. Chim. Acta.*, 297: 191–205, 2000.
- Perrotte, P., Matsumoto, T., Inoue, K., Kuniyasu, H., Eve, B. Y., Hicklin, D. J., Radinsky, R., and Dinney, C. P. Anti-epidermal growth factor receptor antibody C225 inhibits angiogenesis in human transitional cell carcinoma growing orthotopically in nude mice. *Clin. Cancer Res.*, 5: 257–265, 1999.
- Wu, R., L., Osman, I., Wu, X. R., Lu, M. L., Zhang, Z. F., Liang, F. X., Hamza, R., Scher, H., Cordon-Cardo, C., and Sun, T. T. Uroplakin II is expressed in transitional cell carcinoma but not in bilharzial bladder squamous cell carcinoma: alternative pathways of bladder epithelial differentiation and tumor formation. *Cancer Res.*, 58: 1291–1297, 1998.
- Li, S. M., Zhang, Z. T., Chan, S., McLenan, O., Dixon, C., Taneja, S., Lepor, H., Sun, T. T., and Wu, X. R. Detection of circulating uroplakin-positive cells in patients with transitional cell carcinoma of the bladder. *J. Urol.*, 162: 931–935, 1999.
- Reiter, R. E., Gu, Z., Watabe, T., Thomas, G., Szigeti, K., Davis, E., Wahl, M., Nisitani, S., Yamashiro, J., Le Beau, M. M., Loda, M., and Witte, O. Prostate stem cell antigen: a cell surface marker overexpressed in prostate cancer. *Proc. Natl. Acad. Sci. USA*, 95: 1735–1740, 1998.
- Gu, Z., Thomas, G., Yamashiro, J., Shintaku, I. P., Dorey, F., Raitano, A., Witte, O. N., Said, J. W., Loda, M., and Reiter, R. E. Prostate stem cell antigen (PSCA) expression increases with high Gleason score, advanced stage and bone metastasis in prostate cancer. *Oncogene*, 19: 1288–1296, 2000.
- Saffran, D. C., Raitano, A. B., Hubert, R. S., Witte, O. N., Reiter, R. E., and Jakobovits, A. Anti-PSCA monoclonal antibodies inhibit tumor growth and metastasis formation and prolong the survival of mice bearing human prostate cancer xenografts. *Proc. Natl. Acad. Sci. USA*, in press, 2001.
- Dannull, J., Diener, P., Prikler, L., Furstenberger, G., Cerny, T., Schmid, U., Ackermann, D. K., and Gorettrup, M. Prostate stem cell antigen is a promising candidate for immunotherapy of advanced prostate cancer. *Cancer Res.*, 60: 5522–5528, 2000.
- Said, J. W., Pinkus, J. L., Shintaku, I. P., deVos, S., Matsumura, F., Yamashiro, S., and Pinkus, J. S. Alterations in fascin expressing germinal center dendritic cells in neoplastic follicles of B-cell lymphomas. *Mod. Pathol.*, 11: 1–5, 1998.
- Hanas, J. S., Lerner, M. R., Lightfoot, S. A., Raczkowski, C., Kastens, D. J., Brackett, D. J., and Postier, R. G. Expression of the cyclin-dependent kinase inhibitor p21

⁵ T. Watabe, R. E. Reiter, M. Lin, A. A. Donjacour, G. R. Cunha, and O. N. Witte. *In situ* visualization of a growth responsive subset of epithelial cells associated with prostate development, regeneration and tumorigenesis, submitted for publication.

⁶ Z. Gu and R. E. Reiter, unpublished data.

(WAF1/CIP1) and p53 tumor suppressor in dysplastic progression and adenocarcinoma in Barrett esophagus. *Cancer (Phila.)*, **86**: 756-763, 1999.

14. Sambrook, J., Fritsch, E. F., and Maniatis, T. Extraction, purification, and analysis of messenger RNA from eukaryotic cells. In: *Molecular Cloning*, Ed. 2, pp. 7.3-7.87. Cold Spring Harbor, NY: Cold Spring Harbor Laboratory Press, 1989.

15. Brakenhoff, R. H., Gerretsen, M., Knippels, E. M. C., van Dijk, M., van Essen, H., Weghuis, D. O., Sinke, R. J., Snow, G. B., and van Dongen, G. A. M. S. The human E48 antigen, highly homologous to the murine Ly-6 antigen ThB, is a GPI-anchored molecule apparently involved in keratinocyte cell-cell adhesion. *J. Cell Biol.*, **129**: 1677-1689.

16. Bahrenberg, G., Brauers, A., Joost, H., and Jaske, G. Reduced expression of PSCA, a member of the Ly-6 family of cell surface antigens, in bladder, esophagus, and stomach tumors. *Biochem. Biophys. Res. Comm.*, **273**: 783-788, 2000.

17. Reiter, R. E., Sato, I., Thomas, G., Qian, J., Gu, Z., Watabe, T., Loda, M., and Jenkins, R. B. Coamplification of prostate stem cell antigen (PSCA) and myc in locally advanced prostate cancer. *Genes Chromosomes Cancer*, **00**: 1-9, 1999.

18. Christoph, F., Schmidt, B., Schmitz-Drager, B. J., and Schulz, W. A. Over-expression and amplification of the *c-myc* gene in human urothelial carcinoma. *Int. J. Cancer*, **84**: 169-173, 1999.

19. Sauter, G., Carroll, P., Moch, H., Kallioniemi, A., Kerschmann, R., Narayan, P., Mihatsch, M. J., and Waldman, F. M. C-myc copy number gains in bladder cancer detected by fluorescence *in situ* hybridization. *Am. J. Pathol.*, **146**: 1131-1139, 1995.

20. Hughes, O. D., Bishop, M. C., Perkins, A. C., Wastie, M. L., Denton, G., Price, M. R., Frier, M., Denley, H., Rutherford, R., and Schubiger, P. A. Targeting superficial bladder cancer by the intravesical administration of copper-67 labeled anti-MUC1 mucin monoclonal antibody C595. *J. Clin. Oncol.*, **18**: 363-370, 2000.

Prostate Stem Cell Antigen as Therapy Target: Tissue Expression and *in Vivo* Efficacy of an Immunoconjugate

Sarajane Ross,¹ Susan D. Spencer,¹ Ilona Holcomb, Christine Tan, JoAnne Hongo, Brigitte Devaux, Linda Rangell, Gilbert A. Keller, Peter Schow, Rita M. Steeves, Robert J. Lutz, Gretchen Frantz, Kenneth Hillan, Franklin Peale, Patti Tobin, David Eberhard, Mark A. Rubin, Laurence A. Lasky, and Hartmut Koeppen²

Departments of Pathology [S. R., I. H., G. F., K. H., F. P., P. T., D. E., H. K.], Molecular Oncology [S. D. S., L. A. L.], Antibody Technology [C. T., J. H., B. D.], Toxicology [L. R., G. A. K.], and Immunology [P. S. J., Genentech, Inc., South San Francisco, California 94080; ImmunoGen, Inc., Cambridge, Massachusetts 02139 [R. M. S., R. J. L.]; and Department of Pathology and Urology, University of Michigan, Ann Arbor, Michigan 48109 [M. A. R.]

ABSTRACT

We conducted an expression analysis of prostate stem cell antigen (PSCA) in normal urogenital tissues, benign prostatic hyperplasia ($n = 21$), prostatic intraepithelial neoplasia ($n = 33$), and primary ($n = 137$) and metastatic ($n = 42$) prostate adenocarcinoma, using isotopic *in situ* hybridization on tissue microarrays. In normal prostate, we observe PSCA expression in the terminally differentiated, secretory epithelium; strong expression was also seen in normal urothelium. Forty-eight percent of primary and 64% of metastatic prostatic adenocarcinomas expressed PSCA RNA. Our studies did not confirm a positive correlation between level of PSCA RNA expression and high Gleason grade. We characterized monoclonal anti-PSCA antibodies that recognize PSCA expressed on the surface of live cells, are efficiently internalized after antigen recognition, and kill tumor cells *in vitro* in an antigen-specific fashion upon conjugation with maytansinoid. Unconjugated anti-PSCA antibodies demonstrated efficacy against PSCA-positive tumors by delaying progressive tumor growth *in vivo*. Maytansinoid-conjugated antibodies caused complete regression of established tumors in a large proportion of animals. Our results strongly suggest that maytansinoid-conjugated anti-PSCA monoclonal antibodies should be evaluated as a therapeutic modality for patients with advanced prostate cancer.

INTRODUCTION

Prostate cancer is the most commonly diagnosed nondermatological malignancy in men, and according to the American Cancer Society accounts for 30,000 deaths annually in the United States.³ Whereas primary organ-confined cases can effectively be treated and cured by surgery and/or radiation therapy, therapeutic options are limited for metastatic, hormone-refractory disease (1). The lack of success with conventional therapeutic approaches and the existence of antigens expressed in an almost organ-specific pattern have prompted immunological approaches to the treatment of metastatic prostate cancer. Most of the studies designed to elicit active immunity in the patient are in their early stages and cannot be fully evaluated at this time (2–8).

Antibody-based therapy using unconjugated, toxin-conjugated, or radiolabeled reagents against tumor-associated target antigens has proven beneficial for solid and hematolymphoid neoplasms (for a review, see Ref. 9). Recent clinical efforts have focused on the toxic natural compounds calicheamicin and maytansinoid DM1. Immunoconjugates with these two toxins have shown efficacy with limited toxicity in preclinical studies and are now in various stages of clinical development for hematological and solid tumors (10, 11).

Received 9/27/01; accepted 3/1/02.

The costs of publication of this article were defrayed in part by the payment of page charges. This article must therefore be hereby marked *advertisement* in accordance with 18 U.S.C. Section 1734 solely to indicate this fact.

¹ Sarajane Ross and Susan D. Spencer contributed equally to this work.

² To whom requests for reprints should be addressed, at Genentech, Inc., Mail Stop 72B, 1 DNA Way, South San Francisco, CA 94080. Phone: (650) 225-8134; Fax: (650) 225-8989; E-mail: hkoepen@gene.com.

³ <http://www.cancer.org>.

The present study evaluates PSCA⁴ as a potential target for an antibody-based therapeutic approach against prostate cancer. We describe the expression pattern of PSCA in normal adult urogenital tissues and in primary and metastatic prostate cancer as well as the *in vitro* and *in vivo* characteristics of unconjugated and DM1-conjugated anti-PSCA antibodies. PSCA was originally identified as a glycosylated, glycosylphosphoinositol-linked cell surface antigen expressed in normal prostate, urinary bladder, kidney, and placenta. Expression has also been described in primary and metastatic prostate cancer as well as in neoplasms of the urinary bladder, esophagus, and pancreas by several groups using diverse methodologies (12–14). Here we conclusively show that PSCA is strongly expressed in differentiated luminal cells of the prostate and urothelium. PSCA RNA is present in 48% of primary and 64% of metastatic prostatic adenocarcinomas. In addition, we generated anti-PSCA monoclonal antibodies that specifically reacted with cell surface PSCA and, upon conjugation with maytansinoid DM1, demonstrated *in vitro* cytotoxicity and marked *in vivo* efficacy with complete tumor eradication in a large proportion of treated animals. To our knowledge, this is the first study showing eradication of established xenograft tumors using PSCA as a target in a passive immunotherapy approach.

MATERIALS AND METHODS

TMAs. We used paraffin blocks of normal and neoplastic human tissues from two separate institutions (University of Sheffield, Sheffield, United Kingdom, and University of Virginia, Charlottesville VA) to build two microarrays of prostatic tissue as described previously (15). These two TMAs contained 240 and 294 tissue elements, respectively. Six additional arrays consisting of 144 elements each of normal, hyperplastic, and neoplastic prostate tissues were built at the University of Michigan (Ann Arbor, MI). Tissues were represented in triplicate cores 600 μm in diameter. A detailed description of our TMA and ISH technology has recently been published (16). All cases of prostate cancer had been assigned a Gleason score by the pathologist at the original institution based on histological evaluation of a prostatectomy specimen. The total numbers of cases with normal prostate, PIN, and primary and metastatic prostate cancer are summarized on Table 1. In the category of PIN, we considered only high-grade lesions with the typical architectural and cytological features (17). The sites of metastatic prostate cancer were the lymph nodes ($n = 24$), liver ($n = 9$), lung ($n = 2$), and 1 case each of brain, meninges, diaphragm, kidney, stomach, testis, and soft tissue. We were unable to evaluate skeletal metastases because the decalcification procedure used for bone-containing tissues damages the RNA to an extent that it becomes unsuitable for ISH.⁵ The age range for the patients was 39–82 years.

ISH. PCR primers were designed to amplify a 751-bp fragment of human PSCA corresponding to nucleotides 1–751 of the GenBank sequence (NM_005672). A probe for β -actin was designed to correspond to nucleotides 784–1074 of the human β -actin GenBank sequence (BC004251). Primers

⁴ The abbreviations used are: PSCA, prostate stem cell antigen; TMA, tissue microarray; ISH, *in situ* hybridization; PIN, prostatic intraepithelial neoplasia; BPH, benign prostatic hyperplasia; ATCC, American Type Culture Collection; FBS, fetal bovine serum; CHO, Chinese hamster ovary; EM, electron microscopy.

⁵ S. Ross and H. Koeppen, personal observation.

Table 1 Incidence and intensity of expression of PSCA in human prostate tissue

Type of prostate tissue (No. of samples analyzed)	Incidence according to intensity of expression (%)				
	1+	2+	3+	4+	Total
Normal/BPH (n = 78)	23	10	13	1	47
PIN (n = 33)	12	12	40	12	76
PC, ^a Gleason grade ≤7 (n = 76)	19	16	13	1	49
PC, Gleason grade >7 (n = 61)	20	12	13	3	48
Metastatic PC (n = 42)	29	9	19	7	64

^a PC, prostate cancer.

included extensions encoding 27-nucleotide T7 or T3 RNA polymerase initiation sites to allow *in vitro* transcription of sense or antisense probes, respectively, from the amplified products. Except for a digestion in 20 µg/ml proteinase K at 37°C for 15 min, TMA sections were processed for ISH as described previously (18). Sense control probes showed no signal above background (data not shown).

Scoring and Analysis of TMA PSCA Expression. The intensity of PSCA expression evaluated microscopically was given a score of 0–4, with 4 being the highest expression observed. The percentage of epithelial cells positive for PSCA within a TMA element was estimated as <10%, 10–50%, or >50%. Patients with expression of PSCA in <10% of epithelial cells were considered negative. The intensity score and percentage of positive cells in elements from the same patient were averaged. Pathological diagnoses and ISH results were tabulated using Microsoft Excel.

Immunohistochemistry. Immunohistochemical staining for Ki-67 was performed with a rabbit polyclonal antibody (DAKO Corporation, Carpinteria, CA) on the two in-house-built prostate TMAs according standard procedures and the manufacturer's guidelines. Represented on these two TMAs were 22 normal prostate tissues, 4 cases of BPH, 7 cases of PIN, and 90 primary and 27 metastatic prostatic adenocarcinomas. Antigen retrieval was performed at 99°C for 40 min in Target Retrieval Solution (DAKO). The primary antibody was used at a dilution of 1:100. Cases of prostate cancer were scored according to the percentage of nuclei positive for Ki-67 and separated into four categories: ≤10%, 10–25%, 25–50%, or >50% of the nuclei positive. The Ki-67 score was then compared with the PSCA intensity score, using Statview software (SAS, Inc.). Staining for chromogranin A was performed on a paraffin TMA section with a rabbit polyclonal antibody (DAKO Corporation) at a 1:400 dilution without antigen retrieval.

Recombinant Plasmids and Cell Lines. The following human cell lines were used: PC3 (prostate cancer; gift from E. Sauseville, National Cancer Institute, Bethesda, MD), HCT116 (colon cancer; ATCC, Manassas, VA), SW780 (bladder cancer; ATCC), and MCF7.Her2 (breast cancer; gift from G. P. Lewis, Genentech). All cell lines were grown in 50% Ham's F-12, 50% DMEM supplemented with 10% FBS and penicillin-streptomycin (1000 units/ml; Life Technologies, Inc.) referred to hereafter as complete medium. The PSCA coding sequence (amino acids 16–123) was subcloned into the plasmid pRK.tkneo (19), which was engineered to contain the herpes simplex virus glycoprotein D signal and epitope tag (20). Stable transfectants of CHO, PC3, and HCT116 cell lines expressing human gD.PSCA were generated by Fugene transfection (Roche Molecular Biochemicals, Indianapolis, IN) of pRK.gD.h.PSCA, followed by selection in 400 µg/ml G418. Individual clones were selected and analyzed for PSCA expression. The number of PSCA molecules expressed by the individual cloned cell lines was determined by Scatchard analysis (data not shown) and was as follows: 5,000,000 in PC3.gD.PSCA; 2,500,000 in MCF7.Her2.gD.PSCA; 1,600,000 in HCT116.gD.PSCA clone 6; and 400,000 in HCT116.gD.PSCA clone 8.

Monoclonal Anti-PSCA Antibodies. BALB/c mice (Charles River Laboratories, Wilmington, DE) were immunized with an *Escherichia coli*-derived poly(His)-tagged PSCA polypeptide lacking the NH₂- and COOH-terminal hydrophobic sequences and diluted in Ribi adjuvant (Ribi Immunochem Research, Inc., Hamilton, MO). B cells from the five mice demonstrating high anti-PSCA antibody titers were fused with mouse myeloma cells (X63.Ag8.653; ATCC) as described previously (21, 22). After 10–14 days, the supernatants were harvested and screened for antibody production by direct ELISA and by flow cytometry on CHO.gD.h.PSCA cells. For large-scale production of purified antibody, hybridoma clones were injected i.p. into

pristane-primed mice (23). The ascites fluids were pooled and purified by protein A affinity chromatography (Pharmacia Fast Protein Liquid Chromatography; Pharmacia, Uppsala, Sweden) as described previously (22).

Flow Cytometry. Cells were incubated with primary anti-PSCA monoclonal antibody at a concentration of 20 µg/ml for 1 h on ice and then washed with cold PBS-1% FBS. Specifically bound antibody on the cell surface was detected with a FITC-conjugated goat antimouse IgG. The fluorescence intensity was measured on a Coulter Elite flow cytometer (Coulter Elite-EST; Beckman Coulter, Fullerton, CA).

Preparation of Anti-PSCA-DM1 Immunoconjugate. The conjugation of the anti-PSCA antibody 8D11 and the control antiragweed antibody 10D9 with the maytansinoid toxin DM1 was performed according to the procedure described previously for the antibody C242 (11). 8D11-DM1 contains an average of 3.8 DM1 molecules/antibody molecule. Indicating that the conjugation did not affect the affinity of 8D11, the binding of the conjugated antibody to His-tagged PSCA protein in an ELISA assay was identical to that of the unconjugated antibody (data not shown).

Immunogold Labeling and EM. Transfected cell lines expressing gD.PSCA were grown in 6-well plates and incubated at 4°C with 10 µg/ml anti-gD or anti-PSCA antibody for 1 h. After incubation with primary antibodies, the cells were treated with 10-nm gold adducts of goat antimouse IgG for 1 h. The cells were then switched to 37°C for 1.25 h before fixation in Karnovsky's fixative and processed for EM. For autoradiography, transfected cells were incubated with iodinated anti-PSCA antibodies at 37°C, fixed, washed, and prepared for EM autoradiography as described elsewhere (24). Thin sections were observed in a Philips CM12 equipped with a digitizing GATAN camera.

Antibody Internalization Assay. MCF7.Her2 cells stably transfected with gD.PSCA were grown in 6-well dishes and then incubated at 37°C with 20 nM ¹²⁵I-labeled anti-PSCA and anti-HER2 monoclonal antibodies for 5 h in DMEM supplemented with 10% FBS. To determine the cellular distribution of radiolabeled antibody, the cells were first washed extensively with DMEM and then incubated for 5 min in 2 M urea-50 mM glycine (pH 2.4)-150 mM NaCl. The released radioactivity was considered to represent cell surface-associated antibody. Cells were then solubilized in 8 M urea-150 mM NaCl, and the radioactivity within the lysate was considered to represent internalized antibody. Assays were performed in duplicate wells. The number of antibody molecules bound and internalized per cell was determined on the basis of the specific activity of the iodinated antibody.

In Vitro Cytotoxicity Assay. Tumor cell lines stably transfected with gD.PSCA or with vector alone were plated in 96-well microtiter plates at the following densities in complete medium: 10³ cells/well for HCT116.gD.PSCA, 2 × 10³ cells/well for MCF7.Her2.gD.PSCA, 10³ cells/well for PC3.gD.PSCA, and 1.5 × 10⁴ cells/well for PC3.gD.PSCA. After the cells had been allowed to adhere for 16 h, they were exposed to various concentrations of immunoconjugate 8D11-DM1 (equivalent to 1200 to 0.06 ng/ml DM1). After incubation at 37°C for 7 days, the monolayers were washed twice with PBS and stained with crystal violet dye (0.5% in methanol). The stained cells were solubilized in 50 mM sodium citrate in 50% ethanol for 20 min with shaking. The absorbance at 450 nm (A₄₅₀) of the solubilized cells was measured with a spectrophotometer, and the fraction of surviving cells determined by dividing the A₄₅₀ of treated cells by the A₄₅₀ of nontreated cells. To determine the cytotoxicity of the immunoconjugate on quiescent cells, the assay was performed in serum-free medium.

In Vivo Tumor Growth Assays. Female NCR nude mice (6–8 weeks of age; Taconic, Inc., Germantown, NY) were inoculated s.c. with 5 × 10⁶ PC3.gD.PSCA or 1.5 × 10⁷ SW780 cells. Tumor volume was calculated based on two dimensions, measured using calipers, and was expressed in mm³ according to the formula: V = 0.5a × b², where a and b are the long and the short diameters of the tumor, respectively. Antibody injections were started either 24 h before tumor inoculation or after tumors were established. In the latter type of study, animals were randomized according to tumor volume (mean tumor volume between 100 and 200 mm³) before antibody injections. Unconjugated anti-PSCA and control (antiragweed) antibodies were injected i.p. twice a week at a dose of 10 mg/kg for 4 weeks (unless otherwise indicated). Maytansinoid (DM1)-conjugated antibodies were injected i.v. at a concentration of 75 µg/kg DM1 toxin for the PC3.gD.PSCA tumor model and 150 µg/kg for the SW780 tumor model. Conjugated antibodies were administered twice a week for a total of eight

doses for most studies unless otherwise indicated. Tumors were measured twice a week throughout the experiment. Mice were euthanized before mean tumor volumes reached 2000 mm³ or when tumors showed signs of impending ulceration. All studies were conducted in accordance with the Guide for the Care and Use of Laboratory Animals, published by the NIH (NIH Publication 85-23, revised 1985).

RESULTS

PSCA Expression in Normal Tissues and Prostate Cancer.

PSCA was expressed to various degrees in individual samples of normal prostate. Some areas of prostate expressed very high levels, whereas other areas were completely negative. There was no obvious morphological correlation with level of expression and prostatic region or secretory state. Expression was localized exclusively to the secretory epithelium (Fig. 1, A and B). Basal epithelial cells and prostatic stroma were negative for PSCA RNA in all cases examined (Fig. 1C). Neuroendocrine cells were identified by an immunohistochemical stain for chromogranin A and were negative for PSCA: the distribution and prevalence of chromogranin A-positive cells was quite distinct from that of PSCA-positive cells (Fig. 1D). The RNA integrity of all tissues was confirmed by isotopic ISH with an actin probe (data not shown).

The strongest expression of PSCA RNA in normal urogenital tissues was detected in the urothelium, with equal levels in the renal pelvis, ureter, urinary bladder, and urethra (Fig. 1, E and F). In most areas, the strongest expression was observed in the most superficially located umbrella cells, and the level of expression decreased progressively toward the deeper sections of the mucosa with the lowest expression in the most basally located cells. The stromal tissues of the urinary tract were completely negative for PSCA RNA. In the kidney, scattered PSCA-positive epithelial cells were observed in the distal portions of the collecting system; no expression was noted in the

glomerular tufts or in epithelial cells of proximal collecting ducts and Bowman's capsule.

PSCA Expression in Abnormal Prostate. Expression of PSCA RNA was seen in BPH, PIN, and invasive prostatic adenocarcinoma (Table 1). The phosphorimager scan and image of a representative TMA examined are shown in Fig. 2, A and B, respectively. This TMA included 5 cases of normal urothelium, 4 cases of normal prostate, 4 cases of BPH, 7 cases of PIN, 35 cases of well- and poorly differentiated primary prostate cancer, and 27 cases of metastatic prostate cancer.

As in normal prostate, PSCA expression was restricted to epithelial cells and was focally distributed. The level of expression in the neoplastic prostatic tissues varied from negative to very high. Cases of primary adenocarcinoma were separated into two categories according to Gleason grade: cases with a Gleason grade ≤ 7 , and those with a Gleason grade ≥ 8 . Separation into these two categories has previously been shown to correlate with clinical outcome (25). Cases with metastatic prostate cancer represented a third category. Although expression was variable and no overt correlation with Gleason grade or stage of the disease could be found, the percentage of metastatic prostate cancer cases positive for PSCA was higher (64%) compared with nonmalignant prostate disease and organ-confined prostate cancer (48%; see Table 1). Each case was assigned an intensity score, and patients were grouped according to the level of PSCA expression (Fig. 2, C–J). To determine whether PSCA expression correlated with proliferative activity, we performed immunohistochemical staining for Ki-67 on a subset of cases of primary and metastatic prostate cancer. No correlation was observed between expression of PSCA and expression of Ki-67 (data not shown).

Tumors positive for PSCA RNA were stratified according to signal intensity (1+, 2+, 3+, and 4+) and according to percentage of positive tumor cells (<50% *versus* $\geq 50\%$). Most tumors that scored

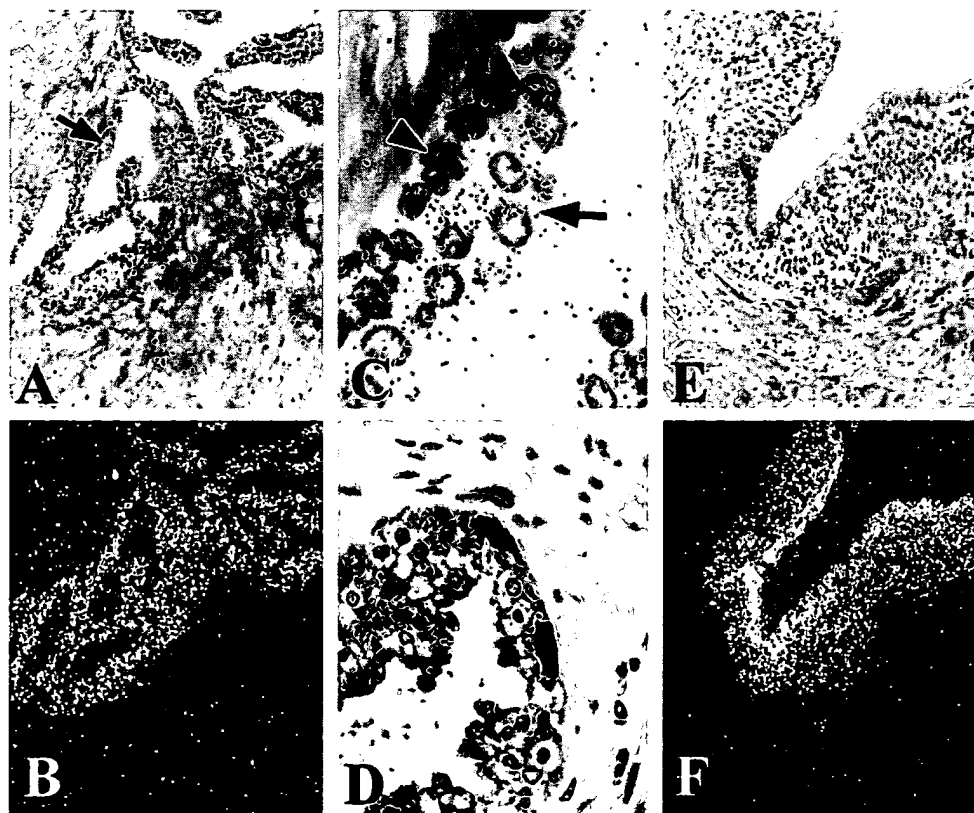


Fig. 1. A–C, PSCA expression in the adult prostate is limited to differentiated, secretory cells. Shown are bright- (A) and darkfield (B) images at $\times 200$ magnification. C, $\times 400$ magnification of the brightfield image in A shows negative basal cells (arrowhead) adjacent to positive secretory cells (arrow). D, immunohistochemical staining for chromogranin A outlines occasional positive neuroendocrine cells within the epithelial cell population (magnification, $\times 400$). E and F, PSCA expression in normal transitional cell mucosa is strongest in superficial cells (magnification, $\times 200$). Bright- (A and E) and darkfield images (B and F) are shown for the same microscopic field.

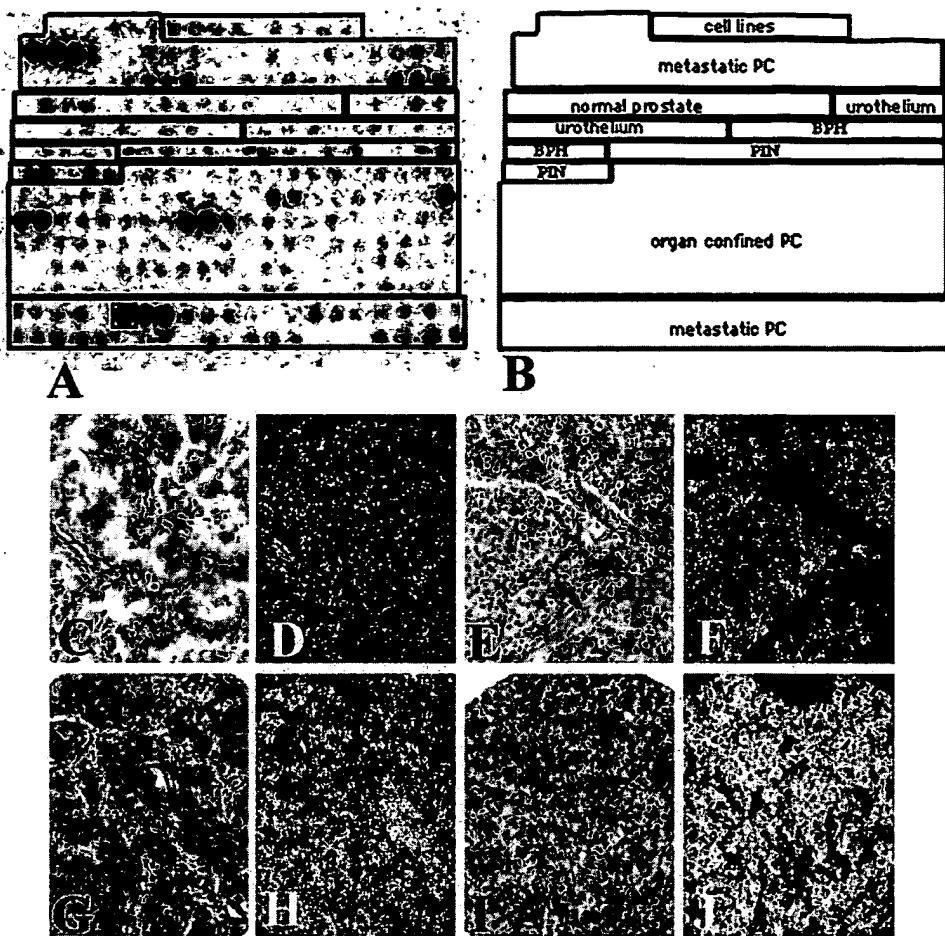


Fig. 2. A, phosphorimager scan of a TMA section after ISH for PSCA. Shown as a representative example is one of the eight prostate TMAs used in this study. Each spot represents a tissue element. Elements are laid out in duplicates or triplicates from a single patient. The darker spots indicate more extensive hybridization of the radioactive probe and correspond to stronger expression of PSCA RNA. B, design of the TMA according to tissue type represented in individual elements. Prostatic tissues include normal, BPH, PIN, and primary and metastatic prostate cancer. C–J, expression of PSCA RNA in primary and metastatic prostatic cancer. Shown are four separate cases representing intensity scores of 1 (C and D), 2 (E and F), 3 (G and H), and 4 (I and J). C–H are cases of primary prostate cancer; I and J show a lymph node metastasis and correspond to the red square in A. Original magnification, $\times 200$ for all images. Bright- (C, E, G, and I) and darkfield images (D, F, H, and J) are shown for the same microscopic field.

positive for PSCA showed expression in the majority of malignant cells ($>50\%$). We did not observe statistically significant differences in the pattern or intensity of PSCA expression between cases with lower and higher Gleason grade or between cases of organ-confined and metastatic disease (data not shown).

Generation and Characterization of Monoclonal Antibodies to PSCA. After an initial screen by ELISA, we identified three monoclonal antibodies (6F8, 8D11, and 5F2) that reacted strongly with PSCA protein on the surface of live cells by flow cytometry using a CHO cell line transfected to express PSCA (data not shown). The affinities of 6F8, 8D11, and 5F2 for His-tagged PSCA were 2.8×10^{-9} M, 3.6×10^{-9} M, and 2.6×10^{-9} M, respectively, as calculated from association and dissociation rate constants measured using a BIACore system. Cross-competition experiments demonstrated that these antibodies recognized the same or overlapping epitopes (data not shown).

Additional cell lines that stably expressed human PSCA after transfection were generated for further *in vitro* and *in vivo* studies. Flow cytometry analysis demonstrated that the anti-PSCA antibody 8D11 specifically recognized PSCA expressed on the surface of four of these cell lines (Fig. 3). None of our antihuman PSCA monoclonal antibodies cross-reacted with murine PSCA (data not shown).

Internalization of Anti-PSCA Antibodies. Two complementary EM techniques, ultrastructural autoradiography and immunogold labeling, were used to identify the internalization pathway of anti-PSCA antibodies. Autoradiographic silver grains were first detected over the villi of transfected cells. Within minutes, the silver grains were observed over flask-shaped invaginations ~ 50 – 100 nm in diameter that resembled caveolae (Fig. 4, A and C). Silver grains were not

associated with coated pits of vesicles. At later time points, the autoradiographic grains were visualized in different organelles of the endosomal compartment (Fig. 4, E–G). Because of the low resolution of the autoradiographic method, we used an immunogold labeling technique to unambiguously discriminate between different cell surface microdomains (see "Materials and Methods" for details). Gold

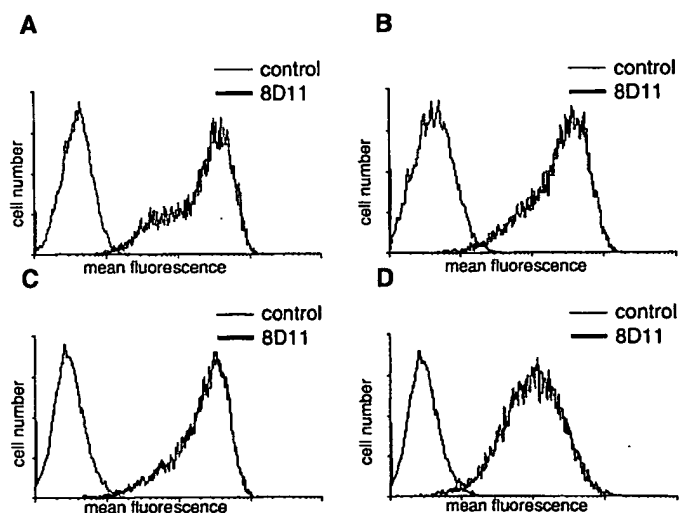


Fig. 3. Cell surface expression of PSCA detected by flow cytometry analysis using the anti-PSCA monoclonal antibody 8D11 (bold lines) or isotype control antibody (light solid lines). Profiles are shown for the four transfected cell lines: PC3.gD.PSCA (A), MCF7.Her2.gD.PSCA (B), and HCT116.gD.PSCA clones 6 (C) and 8 (D).

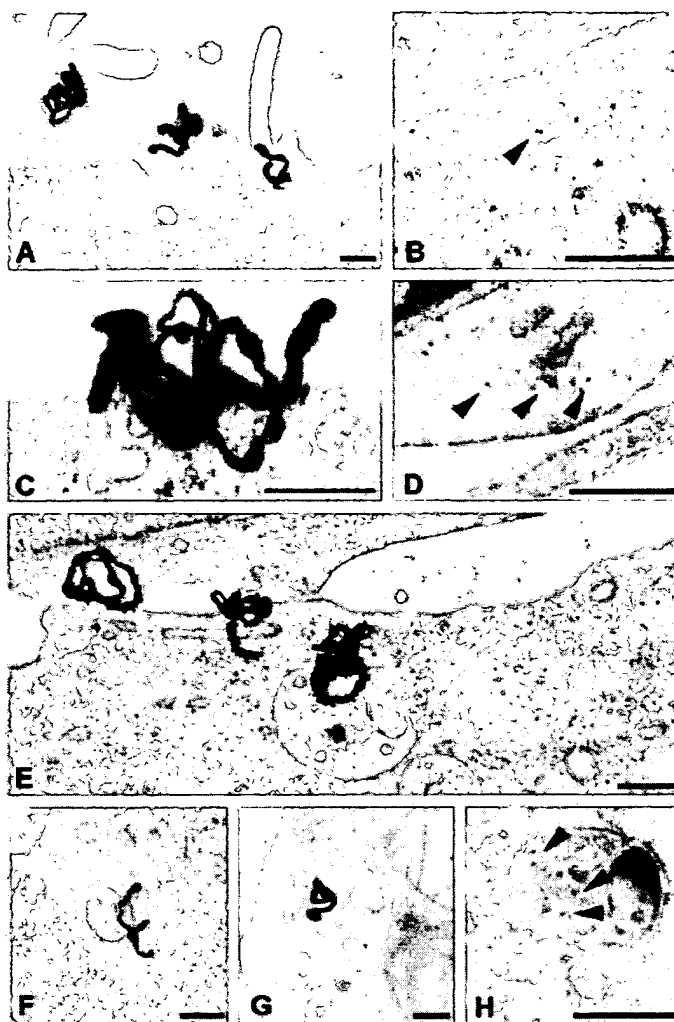


Fig. 4. Internalization of anti-PSCA antibodies in transfected cells visualized by autoradiography (A, C, E, F, and G) and immunogold labeling (B, D, and H). Autoradiographic grains were visualized associated with cell surface projections (A and C) and with endosomes (E–G). Arrowheads indicate gold particles in caveolae (B), in smooth vesicles in the proximal cytoplasm (D), and in a multivesicular body (H).

labels were seen in caveolae-like invaginations and in multivesicular bodies within 20 min after the cells were switched to 37°C (Fig. 4, B, D, and H, arrowheads). These observations suggest that anti-PSCA antibodies were internalized via the caveolae pathway and accumulated within the endolysosomal compartments.

In Vitro Cytotoxicity of Maytansinoid-conjugated Anti-PSCA Antibodies. The cytotoxicity of the DM1-conjugated antibodies was examined using PC3.gD.PSCA and PC3.neo as target cells. As demonstrated in a cell viability assay after a 7-day exposure, the IC_{50} of 8D11-DM1 on PC3.gD.PSCA cells was ~ 1 ng/ml DM1 (equivalent to 3.8×10^{-10} M antibody; Fig. 5C). In comparison, the nonspecific cytotoxicity of 8D11-DM1 on antigen-negative cells was 75-fold lower ($IC_{50} > 75$ ng/ml). In addition, the IC_{50} of the irrelevant control antibody-DM1 conjugate was ~ 75 ng/ml DM1 in both the PC3.gD.PSCA cells and the antigen-negative PC3.neo cells (data not shown).

We also evaluated the cytotoxic potential of 8D11-DM1 in MCF7.Her2.gD.PSCA cells (Fig. 5A) as well as in two subclones of HCT116.gD.PSCA (Fig. 5B) that express different levels of PSCA. 8D11-DM1 killed MCF7.Her2.gD.PSCA with an IC_{50} of 1 ng/ml DM1 and the parental cell line MCF7.Her2 with an IC_{50} of 75 ng/ml DM1. The IC_{50} of 8D11-DM1 in HCT116.gD.PSCA clone 6 ($\sim 1.6 \times 10^6$ receptors/

cell as determined by Scatchard analysis; data not shown) was ~ 6 ng/ml DM1; in clone 8 ($\sim 400,000$ receptors/cell), the IC_{50} was 42 ng/ml DM1. These data show that the cytotoxic effects of the immunoconjugate are observed in an antigen-specific pattern and that the degree of cytotoxicity is dependent on the number of PSCA molecules on the cell surface.

In Vivo Efficacy of Anti-PSCA Antibody against PSCA-positive Tumors. The growth of PSCA-positive tumors was significantly delayed ($P < 0.05$) in animals treated with unconjugated anti-PSCA antibody before tumor cell inoculation compared with animals treated with control antibody (Fig. 6A). Tumors eventually grew, although at a much slower rate than the control treated tumors. In addition, we observed a statistically significant retardation of tumor growth in animals treated with unconjugated anti-PSCA antibodies after tumor establishment compared with animals treated with control antibody ($P < 0.05$). The growth rates of the tumors in the different experimental groups appeared similar after day 20 of the experiment (Fig. 6B).

In subsequent studies we evaluated the efficacy of DM1-conjugated antibodies against established xenograft tumors (average tumor volume at the initiation of therapy, 200 mm^3). Tumor volumes in animals treated with anti-PSCA-DM1 declined after the start of therapy to the extent of complete tumor regression (Fig. 7A). Histological evaluation of the tumor inoculation site at the conclusion of the study, *i.e.*, 30 days after the last injection of antibody, confirmed the absence of viable tumor cells in all eight animals (not shown). As in the study shown, we observed a decrease in tumor volume in the group treated with conjugated control antibody ~ 15 – 25 days after initiation of treatment in several experiments. Fig. 7B shows a study in which efficacy in animals with much larger tumors (average tumor volume, 520 mm^3) was evaluated. Unlike animals treated with conjugated control antibody, the animals treated with the anti-PSCA immunoconjugate showed a continuous decline of tumor volume during the

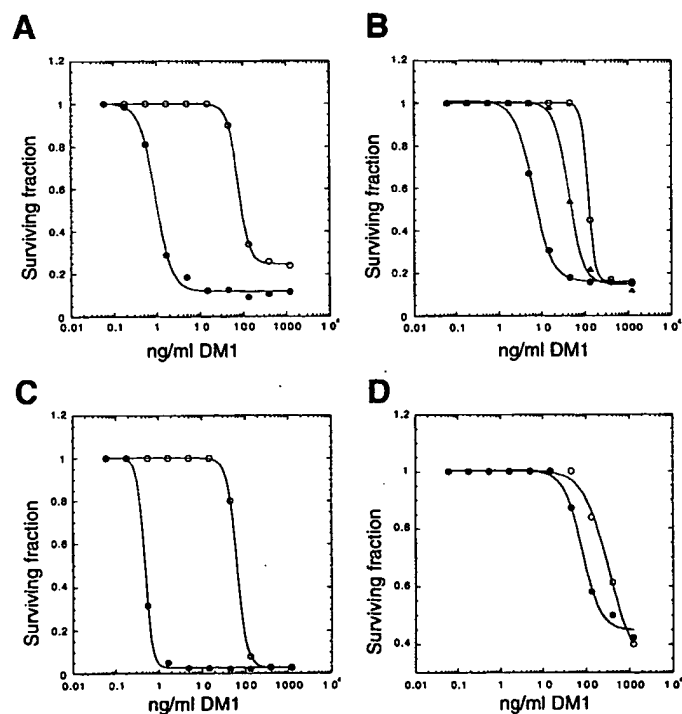


Fig. 5. *In vitro* cytotoxicity of the anti-PSCA immunoconjugate 8D11-DM1. Shown is cell survival as a function of toxin concentration. Assays were performed in serum-containing (A–C) or serum-free (D) tissue culture medium. A, MCF7.Her2.gD.PSCA (●) and MCF7.Her2 (○); B, HCT116.gD.PSCA clone 6 (○), HCT116.gD.PSCA clone 8 (▲), and HCT116 (○); C and D, PC3.gD.PSCA (●) and PC3.neo (○). Data shown are the mean values of quadruplicate analyses.

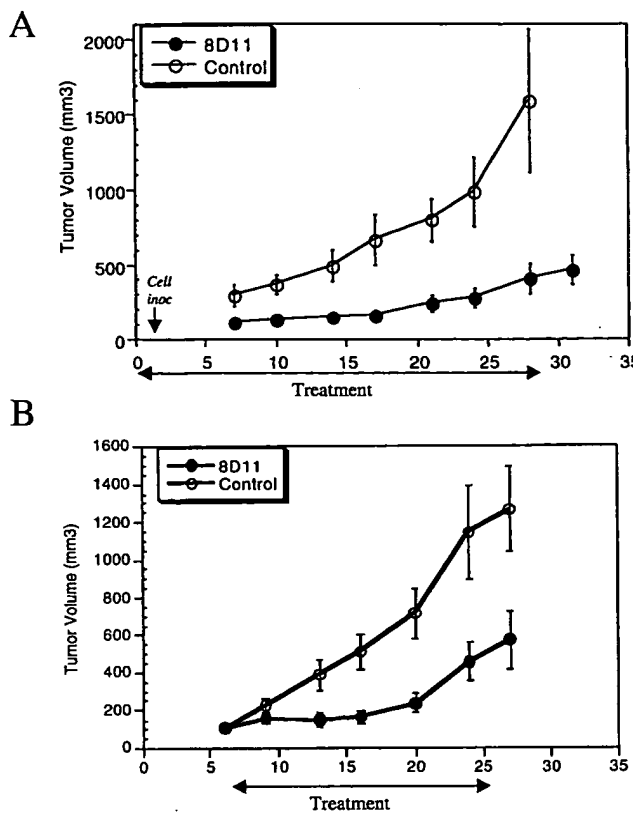


Fig. 6. Antitumor efficacy of unconjugated 8D11 on PC3.gD.PSCA xenografts. Experimental groups in each of the two studies consisted of nine animals, and antibody treatment continued twice a week throughout the course of the experiment as indicated by the horizontal arrow. The first dose of antibody was given either 1 day before tumor cell inoculation (A) or after tumors were established and animals were randomized into two groups based on tumor volume (B). Animals in the control group received an antiragweed monoclonal antibody. Data are shown as mean tumor volume \pm SE (bars).

course of therapy. Therapy was discontinued before macroscopic resolution of the tumor, and all animals evaluated histologically showed residual tumor. However, the *in vivo* measurement of the tumor volume represents an overestimate of the true tumor mass, because the lesions consisted of abundant fibrosis with infiltrates of inflammatory cells as well as nests of viable tumor cells (data not shown). Transfected cells with high levels of PSCA expression were used in the *in vivo* studies described above. To address the issue of whether cells with lower levels of expression are sensitive to anti-PSCA-DM1 therapy, we performed a tumor efficacy study with the bladder cancer cell line SW780. This cell line endogenously expresses PSCA protein at a 10-fold lower level than the PC3.gD.PSCA cell line ($\sim 500,000$ PSCA molecules/cell by Scatchard analysis; data not shown) and exhibits minimal sensitivity in the *in vitro* cytotoxicity assay (data not shown). Treatment of SW780 tumor-bearing animals with DM1-conjugated anti-PSCA antibody resulted in marked retardation of tumor growth, whereas animals treated with control antibody-DM1 showed progressive tumor growth (Fig. 7C). Residual tumors isolated from anti-PSCA-DM1-treated animals still expressed PSCA RNA at the original level as determined by ISH (data not shown).

DISCUSSION

In parallel with our previous characterization of the expression pattern of murine PSCA in normal and neoplastic tissue (18), we performed an expression analysis of the human orthologue in benign and malignant urogenital tissues. Our observations confirm previous

reports (26–28) describing expression in normal and neoplastic prostate tissue, kidney, and bladder. Unlike the original description of expression in the prostatic basal cell compartment, we conclusively show that the terminally differentiated, secretory epithelial cell is the site of expression of PSCA in the prostate. Similarly, in transitional cell mucosa of the urinary tract, expression was strongest in the differentiated, superficial cell population. Whether PSCA should still be considered a “stem cell” antigen based on its distant sequence homology to members of the *Ly-6* gene family, including the stem cell antigens sca-1 and sca-2 (29), should be re-evaluated once the function of this protein has been determined.

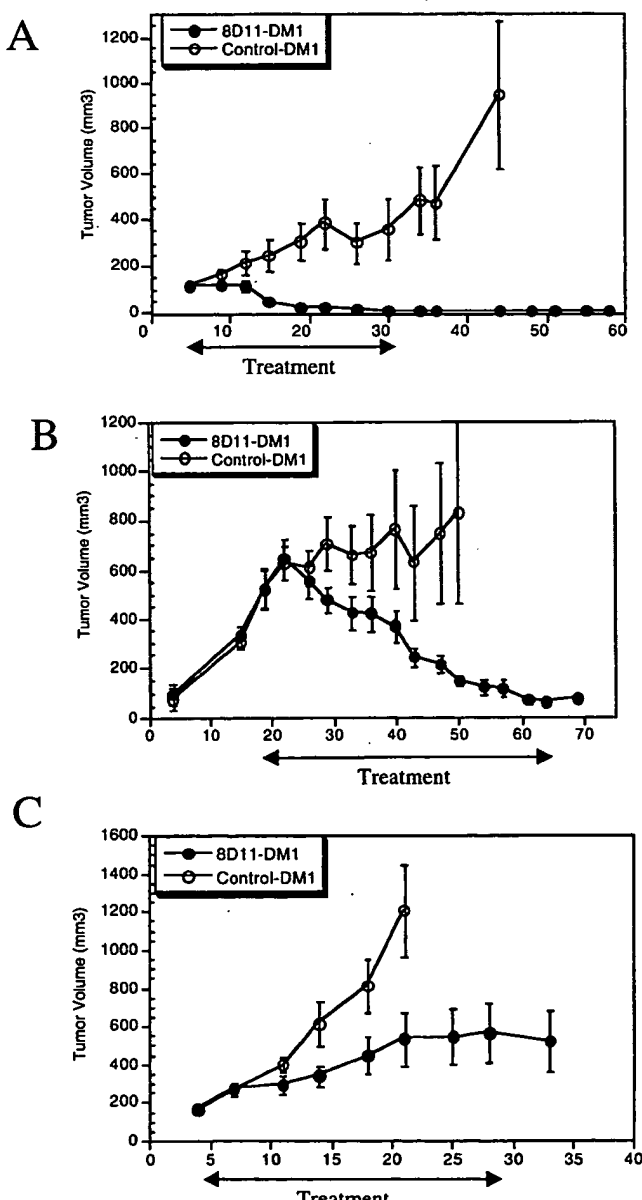


Fig. 7. Antitumor efficacy of DM1-conjugated 8D11 on established PC3.gD.PSCA (A and B) and SW780 xenografts (C). Tumor cells were inoculated on day 0, and the first antibody treatment was given on day 6 (A and C) or day 20 (B) after randomization of animals according to tumor volume. Experimental groups consisted of eight (A and C) or six animals (B). Antibody treatments continued twice a week for a total of 8 (A and C) or 14 doses (B). Animals in the control group were euthanized once tumor volumes exceeded 1500 mm^3 . The immunoconjugates were given at a dose of 75 (A and B) or $150 \mu\text{g}/\text{kg}$ (C) DM1, corresponding to antibody concentrations of 5.5 and 6.1 mg/kg for 8D11 and control antibody, respectively. The DM1 concentration was used to calculate the dose to ensure that animals were exposed to the same amount of DM1 toxin during the course of the experiment. Data are shown as mean tumor volume \pm SE (bars).

As our data show, *PSCA* is not a gene that is uniformly expressed within the secretory epithelium of normal prostate or within the malignant cell population of a prostatic adenocarcinoma. It might be argued that expression analysis using the TMA technology might not be the appropriate tool to determine the incidence of expression of *PSCA* given its sometimes focal expression pattern. Although only a very small portion of the original tissue specimen is available for review, the TMA technology has been valuable for expression profiling of numerous indications (30). Adequate assessment of gene expression can typically be accomplished by sampling three representative areas of a given specimen (30). Essentially all of our cases had been sampled at least three times. Furthermore, we observed a very high concordance in a subset of cases, in which elements of normal or neoplastic tissues had been represented in multiple sets of three (data not shown).

A previous report described up-regulation of *PSCA* in prostate cancer metastatic to bone (28). Although there was a trend toward overexpression in metastatic cases in our series, the differences between the individual groups were not statistically significant. Because decalcification techniques lead to the loss of RNA integrity, we were not able to examine *PSCA* expression by our ISH technique in any bone marrow metastases. The differences in metastatic sites may contribute to any discrepancies in *PSCA* expression between the two studies.

The expression profile of *PSCA* together with the *in vivo* efficacy data suggests that *PSCA* is a promising therapeutic target for *PSCA*-expressing tumors. The two most important aspects in the consideration of toxin-conjugated therapeutic antibodies are potential toxicity and antitumor efficacy. Issues of toxicity can be addressed in our model only to a limited extent because the anti-*PSCA* antibody does not recognize the murine orthologue. Toxin-conjugated antimurine *PSCA* antibodies or a human *PSCA* transgenic or knock-in mouse model would be appropriate tools to evaluate toxicity in a mouse model. The efficacy of the toxin-conjugated anti-*PSCA* antibodies observed in the *in vivo* model should be interpreted in the context of our *in vitro* cytotoxicity studies, which demonstrate the broad concentration range in which DM1-conjugated anti-*PSCA* antibody exhibits antigen-specific cytotoxicity. This observation is consistent with previous studies using the same toxin conjugated to an antibody of different specificity (11) against a different tumor target. Because the therapeutic index for free DM1 is too small for clinical use (31), it is necessary for the intact immunoconjugate to be internalized into the target cell. Using ultrastructural autoradiography, we could show that cell surface bound anti-*PSCA* antibody is internalized. *PSCA* is anchored to the cell surface through a glycosylphosphoinositol linkage, and proteins with this particular linkage have been described as being internalized after engagement with ligand or antibody (32, 33).

DM1 inhibits the polymerization of tubulin into filaments and thus interferes with the formation of the mitotic spindle in mitotically active cells and with axonal transport in neuronal cells. This mechanism of action of DM1 would indicate that epithelial tissues with a rapid cellular turnover are particularly prone to potential side effects. Although free DM1 toxin may account for the temporary growth inhibition of control tumors (see Fig. 7, *A* and *B*) because of its effect on mitotically active cells, we did not observe any *in vivo* toxicity related to free DM1 in normal host tissues. Normal urothelium, which shows the highest levels of *PSCA* RNA in postmitotic, terminally differentiated cells (18), would be an obvious concern in this context. However, we attempted to mimic cellular quiescence in our *in vitro* cytotoxicity assay by performing the assay in serum-free medium. Under those circumstances, cytotoxicity by the immunoconjugate on *PSCA*-positive cells was greatly reduced.

Although the *in vitro* cytotoxicity data are quite informative, they

may lead to underestimation of the *in vivo* efficacy of the immunoconjugate. For example, the immunoconjugate shows limited *in vitro* cytotoxicity on the bladder cancer cell line SW780, which expresses ~500,000 *PSCA* molecules on the cell surface. Nevertheless, there was marked *in vivo* efficacy with the same cell line and the same immunoconjugate. The increased length of exposure in the *in vivo* studies may explain this discrepancy, although additional mechanisms cannot be ruled out.

The efficacy of unconjugated anti-*PSCA* antibodies has now been convincingly demonstrated in two separate studies using independently derived monoclonal antibodies (Ref. 34 and this study). If treatment is started before tumor inoculation, retardation of tumor growth, inhibition of metastatic spread, and prolonged survival are observed (34). Similar, although less dramatic, effects have been observed in models using established tumors (34). The use of an antibody-toxin immunoconjugate in our studies markedly increased the *in vivo* efficacy and caused complete eradication of established tumors in the majority of animals when challenged with a cell line expressing high levels of *PSCA*. We observed significant growth retardation in animals challenged with cells expressing at least 10-fold lower levels of *PSCA*. The inability to achieve tumor eradication in the latter model may be attributable to several possible reasons. We know from ISH experiments that the residual tumors in animals treated with the anti-*PSCA* immunoconjugate still express high levels of *PSCA* RNA (data not shown), excluding the possibility of emerging antigen-loss tumor variants. Length of treatment and antibody dose could be manipulated to achieve increased efficacy in the treatment of tumors with low-level expression of *PSCA*. There is no evidence from our *in vitro* experiments that tumor cells acquire resistance to DM1. Tumor dormancy after continued treatment with the immunoconjugate is another possibility, although we observed mitotic activity in the residual microscopic tumors. Generation of neutralizing antibodies against the therapeutic antibody or against the toxin conjugate is not a consideration in this nude mouse xenograft model.

In summary, our studies illustrate a promising approach for the treatment of *PSCA*-expressing tumors. Advanced hormone-refractory prostate cancer, for which no effective therapies are available at this point, would be an obvious indication. Other tumor types that have been reported to express *PSCA* (35, 36) should be considered as well.

ACKNOWLEDGMENTS

We thank Barbara Wright for help with the immunohistochemistry for Ki-67 and chromogranin A, and the Genentech Histology Laboratory for sectioning of TMA blocks.

REFERENCES

1. Garnick, M. B., and Fair, W. R. Prostate cancer: emerging concepts. Part I. *Ann. Intern. Med.*, **125**: 118–125, 1996.
2. Salgaller, M. L., Lodge, P. A., McLean, J. G., Tjoa, B. A., Loftus, D. J., Ragde, H., Kenny, G. M., Rogers, M., Boynton, A. L., and Murphy, G. P. Report of immune monitoring of prostate cancer patients undergoing T-cell therapy using dendritic cells pulsed with Hla-A2-specific peptides from prostate-specific membrane antigen (Psma). *Prostate*, **35**: 144–151, 1998.
3. Tjoa, B. A., and Murphy, G. P. Progress in active specific immunotherapy of prostate cancer. *Semin. Surg. Oncol.*, **18**: 80–87, 2000.
4. Perry, M. J. A., Hroudka, D., and Dalglish, A. G. Prospects for vaccination in prostate cancer. *Drugs Aging*, **16**: 321–327, 2000.
5. Mincheff, M., Tchakarov, S., Zoubak, S., Loukinov, D., Botev, C., Altankova, I., Georgiev, G., Petrov, S., and Meryman, H. T. Naked DNA and adenoviral immunizations for immunotherapy of prostate cancer: a Phase I/II clinical trial. *Eur. Urol.*, **38**: 208–217, 2000.
6. Small, E. J., Fratesi, P., Reese, D. M., Strang, G., Laus, R., Peshwa, M. V., and Valone, F. H. Immunotherapy of hormone-refractory prostate cancer with antigen-loaded dendritic cells. *J. Clin. Oncol.*, **18**: 3894–3903, 2000.

7. Lodge, P. A., Jones, L. A., Bader, R. A., Murphy, G. P., and Salgaller, M. L. Dendritic cell-based immunotherapy of prostate cancer: immune monitoring of a Phase II clinical trial. *Cancer Res.*, **60**: 829–833, 2000.
8. Eder, J. P., Kantoff, P. W., Roper, K., Xu, G. X., Bubley, G. J., Boyden, J., Gritz, L., Mazzara, G., Oh, W. K., Arlen, P., Tsang, K. Y., Panicali, D., Schliom, J., and Kufe, D. W. A Phase I trial of a recombinant vaccinia virus expressing prostate-specific antigen in advanced prostate cancer. *Clin. Cancer Res.*, **6**: 1632–1638, 2002.
9. Green, M. C., Murray, J. L., and Hortobagyi, G. N. Monoclonal antibody therapy for solid tumors. *Cancer Treat. Rev.*, **26**: 269–286, 2000.
10. Sievers, E. L., Appelbaum, F. R., Spielberger, R. T., Forman, S. J., Flowers, D., Smith, F. O., Shannon-Dorcy, K., Berger, M. S., and Bernstein, I. D. Selective ablation of acute myeloid leukemia using antibody-targeted chemotherapy: a Phase I study of an anti-CD33 calicheamicin immunoconjugate. *Blood*, **93**: 3678–3684, 1999.
11. Liu, C. N., Tadayoni, B. M., Bourret, L. A., Mattocks, K. M., Derr, S. M., Widdison, W. C., Kedersha, N. L., Ariniello, P. D., Goldmacher, V. S., Lambert, J. M., Blattler, W. A., and Chari, R. V. J. Eradication of large colon tumor xenografts by targeted delivery of maytansinoids. *Proc. Natl. Acad. Sci. USA*, **93**: 8618–8623, 1996.
12. Amara, N., Palapattu, G. S., Schrage, M., Gu, Z. N., Thomas, G. V., Dorey, F., Said, J., and Reiter, R. E. Prostate stem cell antigen is overexpressed in human transitional cell carcinoma. *Cancer Res.*, **61**: 4660–4665, 2001.
13. Argani, P., Rosty, C., Reiter, R. E., Wilentz, R. E., Murugesan, S. R., Leach, S. D., Ryu, B. W., Skinner, H. G., Goggins, M., Jaffee, E. M., Yeo, C. J., Cameron, J. L., Kern, S. E., and Hruban, R. H. Discovery of new markers of cancer through serial analysis of gene expression: prostate stem cell antigen is overexpressed in pancreatic adenocarcinoma. *Cancer Res.*, **61**: 4320–4324, 2001.
14. Bahrenberg, G., Brauers, A., Joost, H. G., and Jakse, G. Reduced expression of PSCA, a member of the LY-6 family of cell surface antigens, in bladder, esophagus, and stomach tumors. *Biochem. Biophys. Res. Commun.*, **275**: 783–788, 2000.
15. Kononen, J., Bubendorf, L., Kallioniemi, A., Barlund, M., Schraml, P., Leighton, S., Torhorst, J., Mihatsch, M. J., Sauter, G., and Kallioniemi, O. P. Tissue microarrays for high-throughput molecular profiling of tumor specimens. *Nat. Med.*, **4**: 844–847, 1998.
16. Frantz, G. D., Pham, T. Q., Peale, F. V., and Hillan, K. J. Detection of novel gene expression in paraffin-embedded tissues by isotopic *in situ* hybridization in tissue microarrays. *J. Pathol.*, **195**: 87–96, 2001.
17. Amin, M. B., Ro, J. Y., and Ayala, A. G. *Pathology Annual: Nineteen Ninety-Four, Part 2*, pp. 1–31. East Norwalk, CT: Appleton and Lange, 1994.
18. Ross, S., Spencer, S. D., Lasky, L. A., and Koeppen, H. Selective expression of murine prostate stem cell antigen in fetal and adult tissues and the transgenic adenocarcinoma of the mouse prostate model of prostate carcinogenesis. *Am. J. Pathol.*, **158**: 809–816, 2001.
19. Gorman, C. M., Gies, D. R., McCray, G. Transient production of proteins using an adenovirus transformed cell line. *DNA Protein Eng. Technol.*, **2**: 3–10, 1990.
20. Lasky, L. A., Groopman, J. E., Fennie, C. W., Benz, P. M., Capon, D. J., Dowbenko, D. J., Nakamura, G. R., Nunes, W. M., Renz, M. E., and Berman, P. W. Neutralization of the AIDS retrovirus by antibodies to a recombinant envelope glycoprotein. *Science* (Wash. DC), **233**: 209–212, 1986.
21. Kohler, G., and Milstein, C. Continuous cultures of fused cells secreting antibody of predefined specificity. *Nature (Lond.)*, **256**: 495–497, 1975.
22. Hongo, J. A., Mora-Worms, M., Lucas, C., and Fendly, B. M. Development and characterization of murine monoclonal antibodies to the latency-associated peptide of transforming growth factor β 1. *Hybrdoma*, **14**: 253–260, 1995.
23. Freund, Y. R., and Blair, P. B. Depression of natural killer activity and mitogen responsiveness in mice treated with pristane. *J. Immun.*, **129**: 2826–2830, 1982.
24. Li, W., Fawcett, J., Widmer, H. R., Fielder, P. J., Rabkin, R., and Keller, G. A. Nuclear transport of insulin-like growth factor-I and insulin-like growth factor binding protein-3 in opossum kidney cells. *Endocrinology*, **138**: 1763–1766, 1997.
25. Mills, S. E., Bostwick, D. G., Murphy, W. M., and Weiss, M. A. A symposium on the surgical pathology of the prostate. *Pathol. Annu.*, **25**: 109–158, 1990.
26. Reiter, R. E., Sato, I., Thomas, G., Qian, J. Q., Gu, Z. N., Watabe, T., Loda, M., and Jenkins, R. B. Coamplification of prostate stem cell antigen (PSCA) and MYC in locally advanced prostate cancer. *Genes Chromosomes Cancer*, **27**: 95–103, 2000.
27. Reiter, R. E., Gu, Z., Watabe, T., Thomas, G., Szigeti, K., Davis, E., Wahl, M., Nisitani, S., Yamashiro, J., Le Beau, M. M., Loda, M., and Witte, O. N. Prostate stem cell antigen: a cell surface marker overexpressed in prostate cancer. *Proc. Natl. Acad. Sci. USA*, **95**: 1735–1740, 1998.
28. Gu, Z., Thomas, G., Yamashiro, J., Shintaku, I. P., Dorey, F., Raitano, A., Witte, O. N., Said, J. W., Loda, M., and Reiter, R. E. Prostate stem cell antigen (PSCA) expression increases with high Gleason score, advanced stage and bone metastasis in prostate cancer. *Oncogene*, **19**: 1288–1296, 2000.
29. Noda, S., Kosugi, A., Saitoh, S., Narumiya, S., and Hamaoka, T. Protection from anti-TCR/CD3-induced apoptosis in immature thymocytes by a signal through thymic shared antigen-1/stem cell antigen-2. *J. Exp. Med.*, **183**: 2355–2360, 1996.
30. Camp, R. L., Charette, L. A., and Rimm, D. L. Validation of tissue microarray technology in breast carcinoma. *Lab. Investig.*, **80**: 1943–1949, 2000.
31. Issell, B. F., and Crooke, S. T. Maytansine. *Cancer Treat. Rev.*, **5**: 199–207, 1978.
32. Kitchens, R. L., Wang, P. Y., and Munford, R. S. Bacterial lipopolysaccharide can enter monocytes via two Cd14-dependent pathways. *J. Immunol.*, **161**: 5534–5545, 1998.
33. Miotti, S., Bagnoli, M., Ottone, F., Tomassetti, A., Colnaghi, M. I., and Canevari, S. Simultaneous activity of two different mechanisms of folate transport in ovarian carcinoma cell lines. *J. Cell. Biochem.*, **65**: 479–491, 1997.
34. Saffran, D. C., Raitano, A. B., Hubert, R. S., Witte, O. N., Reiter, R. E., and Jakobovits, A. Anti-PSCA mAbs inhibit tumor growth and metastasis formation and prolong the survival of mice bearing human prostate cancer xenografts. *Proc. Natl. Acad. Sci. USA*, **98**: 2658–2663, 2001.
35. Amara, N., Palapattu, G. S., Schrage, M., Gu, Z., Thomas, G. V., Dorey, F., Said, J., and Reiter, R. E. Prostate stem cell antigen is overexpressed in human transitional cell carcinoma. *Cancer Res.*, **61**: 4660–4665, 2001.
36. Argani, P. R. C., Reiter, R. E., Wilentz, R. E., Murugesan, S. R., Leach, S. D., Ryu, B., Skinner, H. G., Goggins, M., Jaffee, E. M., Yeo, C. J., Cameron, J. L., Kern, S. E., and Hruban, R. H. Discovery of new markers of cancer through serial analysis of gene expression: prostate stem cell antigen is overexpressed in pancreatic adenocarcinoma. *Cancer Res.*, **61**: 4320–4324, 2001.


ClustalW Results
[Sequences](#) [Help](#)
[Retrieval](#) [BLAST2](#) [FASTA](#) [ClustalW](#) [CGC Assembly](#) [Phrap](#) [Translation](#)

Confidential -- Property of Incyte Corporation SeqServer Version 4.6 Jan 2002

1312529CD1_PRT_2_PF-0066-4DIV
 g116027LY6A_MOUSE_Ly-6A.2/Ly-6E.1

CLUSTAL W (1.7) Multiple Sequence Alignments

Sequence format is Pearson

 Sequence 1: 1312529CD1_PRT_2_PF-0066-4DIV 123 aa
 Sequence 2: g116027LY6A_MOUSE_Ly-6A.2/Ly-6 134 aa

Start of Pairwise alignments

Aligning...

Sequences (1:2) Aligned. Score: 17

Start of Multiple Alignment

There are 1 groups

Aligning...

Group 1: Delayed

Sequence:1 Score:0

Sequence:2 Score:860

Alignment Score 92

CLUSTAL-Alignment file created [baaBXayPH.aln]

CLUSTAL W (1.7) multiple sequence alignment

 1312529CD1_PRT_2_PF-0066-4DIV
 g116027LY6A_MOUSE_Ly-6A.2/Ly-6

 -----MKAVLLALLMAGLALQPGTALLCYSCAKQVSNECLQVENCT
 MDTSHHTKSCLLILLVALLCAERAQGLECYQCYGVPFETSCPSIT-CP
 *: * * * : * . : . * * . . : * . : * . : *

 1312529CD1_PRT_2_PF-0066-4DIV
 g116027LY6A_MOUSE_Ly-6A.2/Ly-6

 GEQCWT---ARIRAVGLLTVISKGCSLNCVDDSQDYYVG---KKNIT
 DGVCVTQEAAVIVDSQTRKVKNNLCLPICPPNIESMEILGKVNWKTS
 . * * * * . * . : * * : : . : : : :

 1312529CD1_PRT_2_PF-0066-4DIV
 g116027LY6A_MOUSE_Ly-6A.2/Ly-6

 DTDLCNXSGAHALQPAAAILALLPALGLLLWGPQQL
 QEDLCNVAVPNGGSTWTMAGVLLFSSSVLLQTLL-
 : * * * : . . . : . * * : * . : *

 Submit sequences to: